USING BREATH-HOLD HYPERCAPNIA TO SCALE THE FMRI BOLD RESPONSE TO VISUAL STIMULATION IN OLDER ADULTS WITH CARDIOVASCULAR DISEASE

by

NICOLETTE FRANÇOISE SCHWARZ

(Under the Direction of Lawrence H. Sweet)

ABSTRACT

Cardiovascular Disease (CVD) is a heart and blood vessel disease, and has been associated with deterioration in brain function and structure. These alterations, in turn, are implicated in the cognitive decline that can be observed in individuals with CVD. Functional magnetic resonance imaging (fMRI) is a powerful tool used to investigate cognition in older adult populations. However, the blood-oxygenation-level-dependent signal (BOLD) measured with fMRI is sensitive to variations in cerebral blood flow and volume. Impaired cardiovascular health may affect the validity of fMRI and complicate the interpretation of fMRI results. Hypercapnia challenges such as breath-holding can be used to evaluate cerebrovascular reactivity and the resulting estimates can be used as a scaling factor. The current investigation examined the effects of breath-hold hypercapnia scaling of brain activation in response to visual stimulation in a group of fourteen older adults with CVD (mean age=70±9, 3 women) and 14 age-matched healthy older adults (67±7, 8 women). In functional regions of interest, hypotheses were tested that scaling reduces activation magnitude, spatial extent, and variability. Additional exploratory analyses were carried out on the whole brain to

investigate global effects. Hypothesis-testing yielded mixed results with brain activation estimates to visual stimulation being significantly reduced after scaling, while potential changes in activation extent could not be investigated due to spuriously high percent signal changes after scaling. These spurious values also resulted in increased variability. At the whole-brain level, evidence for scaling-induced reductions in visual stimulation amplitude, extent, and variability were observed, and a cluster of significantly different brain activation between groups revealed only after scaling. The global application of this correction method may be useful in detecting regions sensitive to vascular artifacts, including those in task-positive and task-negative networks as well as sinuses. The present findings highlight that conclusions derived from BOLD fMRI studies in older adult populations need to be cautiously interpreted and provide evidence for the utility and feasibility of incorporating a simple hypercapnia-based correction method in routine fMRI pipelines.

INDEX WORDS: Functional Magnetic Resonance Imaging, fMRI, Cardiovascular Disease, CVD, Cerebrovascular Reactivity, Breath-hold Hypercapnia

USING BREATH-HOLD HYPERCAPNIA TO SCALE THE FMRI BOLD RESPONSE TO VISUAL STIMULATION IN OLDER ADULTS WITH CARDIOVASCULAR DISEASE

by

NICOLETTE FRANÇOISE SCHWARZ

B.S., Northwestern University, 2007

M.S., The University of Georgia, 2013

A Dissertation Submitted to the Graduate Faculty of The University of Georgia in Partial Fulfillment of the Requirements for the Degree

DOCTOR OF PHILOSOPHY

ATHENS, GEORGIA

2015

USING BREATH-HOLD HYPERCAPNIA TO SCALE THE FMRI BOLD RESPONSE TO VISUAL STIMULATION IN OLDER ADULTS WITH CARDIOVASCULAR DISEASE

by

NICOLETTE FRANÇOISE SCHWARZ

Major Professor:	Lawrence H. Sweet
Committee:	Nicole A. Lazar
	L. Stephen Miller

Electronic Version Approved:

Suzanne Barbour
Dean of the Graduate School
The University of Georgia
August 2015

DEDICATION

Für meine Mutter Marlen Gretlies Frieda Schwarz

und

meine Großeltern Oda-Maria Veronika Luise und Heinz Ernst Johannes Schwarz.

ACKNOWLEDGEMENTS

I would like to thank Dr. Lawrence H. Sweet, my major advisor and dissertation committee chair, for giving me the freedom to choose this topic in this population; neither of which I had expected to study but both of which have set me on the path I have wanted to pursue. For this, his support and guidance (und gelegentlichen Gedankenaustausch auf Deutsch), I will be forever grateful. I would also like to thank the other members of my dissertation committee, Dr. Nicole A. Lazar and Dr. L. Stephen Miller, for their support and suggestions during the preparation of this dissertation. In particular, I would like to thank Dr. Lazar for the manifold opportunities to learn more about imaging statistics – be it in group meetings or collaborating on a very different yet so similar project to this dissertation.

In addition, I would like to express my gratitude to the Franklin Foundation for their continuous and generous support over the past five years in the form of travel funding, which enabled me to participate in workshops, and national and international conferences which have furthered my research career.

Finally, this study was funded by a RO1 HL084178-01 grant provided by the National Heart, Lung, and Blood Institute.

TABLE OF CONTENTS

LIST OF TABLES

Page

LIST OF FIGURES

Page

CHAPTER 1

INTRODUCTION

Cardiovascular Disease

Cardiovascular Disease (CVD) is the leading cause of death worldwide and in the United States of America (USA), where approximately 85.6 million people live with some form of CVD (Mozaffarian et al., 2015). CVD is a heart and blood vessel disease that comprises various pathological conditions such as ischemic and hemorrhagic stroke, myocardial infarction, heart failure, atherosclerosis, coronary and carotid artery disease, and arrhythmia. Systemic cardiac and vascular dysfunctions associated with CVD are known risk factors that may predispose individuals to cerebrovascular disease (Cohen & Gunstad, 2009). Cerebrovascular disease refers to bleeding (e.g., hemorrhagic stroke) or impaired perfusion (e.g., transient ischemic attack) of the brain that is related to dysfunction of the cerebral vasculature; it is the fourth leading cause of death in the USA (S. L. Murphy, Xu, & Kochanek, 2013). CVD and cerebrovascular disease share common pathophysiology and comorbidity, including several medical conditions that have increased prevalence in the population of the USA, such as hypertension, diabetes, obesity, and smoking (Mozaffarian et al., 2015). They are highly associated and are known causes of impairments in the structural and functional integrity of the brain, and consequently they have been increasingly implicated in cognitive decline (Alosco et al., 2013; Cohen et al., 2009; Irani et al., 2009; Jefferson et

al., 2007; Last et al., 2007; Leritz et al., 2011; Meusel et al., 2014; Tchistiakova, Anderson, Greenwood, & MacIntosh, 2014).

In contrast to the imminent effects of large vessel stroke, these conditions accumulate burden over years, affecting brain function at sub-clinical levels, often before cognitive deficits are recognized (Dharmashankar & Widlansky, 2010; Knopman et al., 2001). Several potential cardiac and peripheral vascular mechanisms, including systemic hypoperfusion (e.g., cardiac output and ejection fraction) (Cohen & Gunstad, 2009; Cohen et al., 2009; Irani et al., 2009), endothelial dysfunction (e.g., brachial artery response) (Dharmashankar & Widlansky, 2010), as well as atherosclerosis (Haley et al., 2007) and cerebral amyloid angiopathy (Peca et al., 2013), have been identified by which CVD may lead to cerebrovascular dysfunction. Heart failure with reduced cardiac output may result in hypoperfusion of blood to the body and subsequently the brain (Georgiadis et al., 2000). The brain critically depends on continuous blood flow and it is normally equipped to ensure adequate perfusion by ways of cerebrovascular autoregulation, that is, by adjusting cerebral vasodilation and vasoconstriction in response to fluctuations in arterial pressure (Iadecola, 2004). Cerebral autoregulation is essential, as brain function ceases within seconds and irreversible damage occurs within minutes if cerebral blood flow is interrupted. If perfusion pressure is low, cerebral arterioles dilate to increase blood flow. In the case of chronic hypoperfusion, however, the prolonged maximal dilation leads to cerebrovascular injury (Cohen & Gunstad, 2009). Similarly, cholesterolemia, hypertension, and diabetes, which occur in more than 43%, 33%, and 21% of the population in the USA (Mozaffarian et al., 2015) respectively, are associated with vascular endothelial dysfunction, narrowing and

stiffening of the vasculature, and breakdown in vessel wall permeability (Dharmashankar & Widlansky, 2010; Flück et al., 2014; Girouard & Iadecola, 2006; Last et al., 2007; Meusel et al., 2014; Tchistiakova et al., 2014). These pathologies can be irreversible and may lead to deficiencies in cerebral autoregulation over time. Deterioration in the autoregulatory system and subsequent undersupply in oxygen and nutrients to the brain are implicated in neural dysfunction and white matter damage, and are a potential mechanism for the etiology of observed cognitive problems (Alosco et al., 2013; Cohen et al., 2009; Haley et al., 2007; Irani et al., 2009; Jefferson et al., 2014; Jefferson et al., 2011; Leritz et al., 2011; Meusel et al., 2014). The heterogeneity of risk factors, pathologies, and comorbidities associated with CVD and cerebrovascular disease complicate research investigating the various structural and functional consequences on an individual's brain and behavior.

Cognitive symptoms associated with CVD and cerebrovascular disease can range from sub-clinical deficits to profound cognitive deterioration, and in severe cases, may ultimately result in vascular dementia, even without a history of large vessel stroke (Cohen & Gunstad, 2009). Upon neuropsychological testing, deficits associated with CVD are typically reported in the cognitive domains of attention, executive function, and processing speed (Cohen et al., 2009); however, other domains may be affected as well (Miller et al., 2012). There is evidence that vascular pathology plays a considerable role in Alzheimer's disease as well (Iadecola, 2004). This cognitive decline can disturb daily functioning, quality of life, physical and mental health status, and treatment efficacy (Belardinelli, Georgiou, Cianci, & Purcaro, 1999; Cohen & Gunstad, 2009). Importantly, many of the aforementioned risk factors occur in healthy aging with similar but more

subtle effects on the brain and cognition, and as such, the risk of cognitive impairment exists even in those who do not have a clinical diagnosis (Flück et al., 2014; Knopman et al., 2001; Last et al., 2007; Leritz et al., 2011; Meusel et al., 2014).

Functional Magnetic Resonance Imaging

A key method to investigate brain function in aging and disease is provided by functional magnetic resonance imaging (fMRI) (D'Esposito, Deouell, & Gazzaley, 2003; Hedden & Gabrieli, 2004; Iadecola, 2004; Samanez-Larkin & D'Esposito, 2008). Magnitude, location, and extent of brain activation in response to cognitive challenges can be non-invasively studied using fMRI. With the ever increasing application of this technology in research settings, it has become critical to identify potential limitations of fMRI when utilized in patient populations (Cohen & Sweet, 2010; D'Esposito et al., 2003).

The blood oxygenation level-dependent (BOLD) signal measured with fMRI is sensitive to variations in cerebral blood flow, cerebral blood volume, and cerebral oxygen metabolism that occur in response to neuronal activity (Heeger & Ress, 2002). An increase in local neuronal activity leads to an increase in local metabolic demand, inducing an inflow of blood to deliver oxygen and nutrients to the site of action. For reasons currently not well understood, this influx of oxygenated blood is much greater than required for oxygen consumption and metabolic rate. Importantly, this oversupply of fresh blood changes the ratio of oxyhemoglobin to deoxyhemoglobin content in the nearby vasculature. The BOLD signal is mainly related to these variations taking place in the arteriole, capillary, and venous vascular bed (Menon, 2001). BOLD fMRI essentially uses the paramagnetic properties of deoxyhemoglobin as an endogenous

contrast agent (Heeger & Ress, 2002). Oxyhemoglobin is slightly diamagnetic and has little effect on the surrounding magnetic field. In contrast, deoxyhemglobin is paramagnetic and causes magnetic field inhomogeneities, which decreases the BOLD signal. Therefore, the large inflow of oxygenated blood in response to increased metabolic demand coinciding with neural activity results in a subsequent increase in the BOLD signal that is due to a wash-out effect of deoxyhemoglobin concentration relative to oxyhemoglobin. The close temporal and spatial proximity of neuronal activity and corresponding changes in hemodynamics, termed neurovascular coupling, are exploited to investigate brain function (Girouard & Iadecola, 2006; Heeger & Ress, 2002; Menon, 2001). Ultimately, however, the dependence of BOLD fMRI on vascular factors remains an important limitation for inferences, especially in older adults and patients with CVD (Iadecola, 2004).

FMRI in Older Adults

Relative to younger adults, healthy older adults exhibit BOLD responses that are lower in percent signal change, have reduced signal-to-noise ratios, and are smaller in spatial activation extent during sensory-motor tasks (Ances et al., 2009; Buckner, Snyder, Sanders, Raichle, & Morris, 2000; D'Esposito, Zarahn, Aguirre, & Rypma, 1999; Gauthier et al., 2013; Hesselmann et al., 2001; Huettel, Singerman, & McCarthy, 2001; Riecker et al., 2003). This has also been demonstrated during cognitive paradigms (Handwerker, Gazzaley, Inglis, & D'Esposito, 2007; Kannurpatti, Motes, Rypma, & Biswal, 2010). These findings have been frequently interpreted as the consequence of normal age-related decline in neural function associated with sensory, motor, and cognitive functions. However, age-related differences in neurovascular coupling may

also influence these results (Buckner et al., 2000; D'Esposito et al., 1999; Handwerker et al., 2007; Huettel et al., 2001). For instance, inefficiencies in vasomotor reactivity of the cerebrovasculature in older adults might produce a delayed BOLD response despite comparable neuronal computation (Riecker et al., 2003). Such a mismatch between the actual signal and a canonical hemodynamic response model used to identify brain activity during fMRI could not only generate a smaller BOLD percent signal change, but could also reduce the spatial extent of activation clusters, because fewer voxels (i.e., the typical unit of analysis) would pass a given significance threshold. Research employing visual, motor, and cognitive paradigms has provided compelling evidence that both neural and vascular sources contribute to observed brain activation differences between healthy older and younger adult groups (Ances et al., 2009; Gauthier et al., 2013; Handwerker et al., 2007; Kannurpatti et al., 2010).

Visual stimulation (VS) paradigms were among the earliest used for fMRI brain mapping and investigations of BOLD mechanisms, as the location of visual cortex is consistent across participants and brain activation patterns are reproducible across a variety of healthy and clinical populations (Bandettini & Wong, 1997; Corfield, Murphy, Josephs, Adams, & Turner, 2001; Donahue et al., 2009; Gati, Menon, Ugurbil, & Rutt, 1997). VS induces robust changes in brain activation in task-positive as well as task-negative networks, which provide complementary information on brain function and cognitive decline. The pattern of reduced BOLD intensity and spatial activation extent in healthy older adults has been observed during VS (Ances et al., 2009; Gauthier et al., 2013; Huettel et al., 2001), and has been extended to older adults with dementia (Buckner et al., 2000) and CVD (Dumas et al., 2012; Peca et al., 2013). Reductions in

baseline cerebral blood flow may underlie a smaller BOLD response in these studies, as fractional cerebral blood flow and cerebral metabolic rate of oxygen were not significantly different in healthy older adults relative to younger adults in one study (Ances et al., 2009). In contrast, a group of older adults with cerebral amyloid angiopathy showed a significantly reduced BOLD response to VS relative to healthy older adults, but did not significantly differ in baseline cerebral blood flow in visual cortex (Dumas et al., 2012). This finding suggests that small vessel damage associated with cerebral amyloid angiopathy may be reflected in reduced vascular response to changes in local metabolic demand but not in resting cerebral blood flow.

FMRI and Cerebrovascular Health

Cerebral blood flow, volume, and perfusion are known to vary with age and disease (D'Esposito et al., 2003; Girouard & Iadecola, 2006; Iadecola, 2004; Samanez-Larkin & D'Esposito, 2008), and it has been demonstrated that these hemodynamic processes underlying the sensitivity of the BOLD contrast vary as a function of cardiovascular health status (Dumas et al., 2012; Last et al., 2007; Peca et al., 2013; Rossini et al., 2004; Röther et al., 2002; Van der Zande, Hofman, & Backes, 2005). Therefore, cerebrovascular dysfunction may affect the validity of fMRI and complicate the interpretation of fMRI results by interfering with the spatiotemporal coupling of neural activity and associated hemodynamic changes (D'Esposito et al., 2003; Girouard & Iadecola, 2006; Iadecola, 2004). Neurovascular decoupling has been observed in healthy older adults (Kastrup, Dichgans, Niemeier, & Schabet, 1998; Riecker et al., 2003), patients with cerebrovascular disease (Hamzei, Knab, Weiller, & Röther, 2003; Peca et al., 2013; Pineiro, Pendlebury, Johansen-Berg, & Matthews, 2002), and

patients with severe CVD (Krainik, Hund-Georgiadis, Zysset, & von Cramon, 2005; Rossini et al., 2004; Röther et al., 2002). Specifically, lower BOLD percent signal change, despite comparable neural response to healthy control groups, has been reported during simple visual and motor tasks in patients with cerebral amyloid angiopathy (Peca et al., 2013), extra-and intra-cranial artery disease (Hamzei et al., 2003), and subcortical stroke (Pineiro et al., 2002). These findings provide evidence that a reduction in BOLD percent signal change may be, in part, due to impaired cerebrovascular reactivity (CVR) that alters blood flow, rather than simply less neural computation that elicits less cerebral blood flow. Indeed, a negative BOLD response lasting throughout normal performance of a motor task has been reported in a patient with extra-cranial artery disease, and demonstrated a prolonged uncoupling of neural activity and cerebral blood flow (Röther et al., 2002). In the absence of a hemodynamic response, continuous oxygen consumption in response to ongoing task-related neural activity would lead to an abnormally prolonged increase in deoxyhemoglobin, and a sustained task-related negative BOLD signal. Importantly, this finding demonstrates that an absent BOLD response does not preclude intact neural function but may be due to severely impaired CVR. Taken together, age- and disease-related deterioration in the cerebrovascular system are likely to affect neurovascular coupling, complicating the validity and interpretation of fMRI results (Girouard & Iadecola, 2006; Rossini et al., 2004).

Cerebrovascular Reactivity

CVR refers to the dilatory capacity of the vasculature, and corresponding changes in cerebral blood flow, in response to a vasoactive stimulus. CVR is an

essential mechanism to maintain constant cerebral blood flow and brain perfusion. Disturbances in CVR secondary to CVD may directly alter the BOLD response, independent of neural or cognitive dysfunction. Lower CVR has been observed in healthy older adults (Gauthier et al., 2013; Kannurpatti et al., 2010; Kastrup et al., 1998; Riecker et al., 2003) and CVD patients (Leoni et al., 2012). CVR severity (i.e., lower CVR) in CVD patients is related to an increased risk of stroke, transient ischemic attack (H. Markus & Cullinane, 2001; Silvestrini et al., 2000), and mortality (Portegies, de Bruijn, Hofman, Koudstaal, & Ikram, 2014). CVD-related heterogeneity in vasomotor reactivity is likely a methodological confound in BOLD fMRI studies in this population; such studies may benefit from controlling for dysfunction in CVR.

Breath-hold Hypercapnia

Hypercapnia challenges can be used to quantify CVR (Fierstra et al., 2013; Mark, Mazerolle, & Chen, 2015). Carbon dioxide (CO_2) induces vasodilation and has been employed as a hypercapnic agent via CO_2 administration or breath-hold (BH) paradigms (Fierstra et al., 2013; Mark et al., 2015; Tancredi & Hoge, 2013). BH prevents elimination of CO_2, resulting in an increase in arterial partial pressure of CO_2 and subsequent increase in cerebral blood flow (Fierstra et al., 2013; Mark et al., 2015). Although hypercapnia triggers a global increase in cerebral blood flow, this increase varies among brain regions. Under the assumption of little or no metabolic change during the BH hypercapnia induction, it is local vasomotor reactivity that causes the influx in oxygenated blood and subsequent increase in the BOLD signal.

BH blocks of 10 seconds have been shown to elicit a significant BOLD effect (Liu, Huang, Wu, & Hsu, 2002). In investigations of breathing as a potential confound in

BOLD fMRI studies, even shorter amounts of three seconds have resulted in significant activation patterns that could be mistaken for task-related activation (Abbott, Opdam, Briellmann, & Jackson, 2005; Birn, Murphy, Handwerker, & Bandettini, 2009). Typically, longer BH blocks result in stronger, more reliable, and more reproducible magnitudes, as well as greater activation extents (Liu et al., 2002; Magon et al., 2009; Stillman, Hu, & Jerosch-Herold, 1995). Prior studies frequently employed block durations between 15 and 40 seconds. Different BH techniques appear to influence BOLD characteristics such as shape (e.g., delay, rise, and duration), magnitude, and variability (Li, Kastrup, Takahashi, & Moseley, 1999; Thomason & Glover, 2008). Breathing depth, volume, and rate all affect the BOLD signal to BH (Birn, Smith, Jones, & Bandettini, 2008; Thomason & Glover, 2008). For example, whether inspiration or expiration precedes holding one's breath affects cerebral blood flow and the shape of the BOLD signal (Leoni, Mazzeto-Betti, Andrade, & de Araujo, 2008; Li et al., 1999; Magon et al., 2009). BH after expiration elicits a BOLD response that directly increases above baseline. In contrast, BH after inspiration results in a biphasic BOLD change, in which there is an initial decrease below baseline and then a delayed response with sluggish trajectory. Individual differences in task performance can be a source of considerable variability among participants. Variance in BOLD percent signal change and in end-tidal partial pressure of CO_2 change can be reduced by having participants control inspiration depth (Birn et al., 2009; Birn et al., 2008; Thomason & Glover, 2008) or follow paced breathing rhythms (e.g., using a metronome) during control blocks (Tancredi & Hoge, 2013; Wilson, 2014).

Like the hemodynamic response during task-related BOLD fMRI, BH hypercapnia also results in regional variation. Significantly larger BOLD responses to BH blocks have been observed in cerebellum and visual cortex relative to frontal regions and basal ganglia in healthy young adults (Kastrup, Kruger, Glover, Neumann-Haefelin, & Moseley, 1999). Primary visual cortex, precuneus, and posterior cingulate gyrus have been shown especially sensitive to cued breathing variations (Abbott et al., 2005; Birn et al., 2009; Birn et al., 2008; Stillman et al., 1995; Thomason & Glover, 2008). Regional differences in vascular density and sinuses (e.g., sagittal and transverse sinuses) contribute to the BOLD response by enhancing the percent signal change in voxels containing draining veins and sinuses (Kastrup, Kruger, Glover, Neumann-Haefelin, et al., 1999; Wilson, 2014). Importantly, this augmentation in the percent signal change is not only true for BH BOLD, but for task-related BOLD as well. Voxels with higher resting state cerebral blood volume (e.g., draining veins) will register a greater signal change relative to voxels with less resting state cerebral blood volume (e.g., grey matter) under identical oxygenation changes in vessels contained in these voxels (Bandettini & Wong, 1997; C. Chang, Thomason, & Glover, 2008; Li et al., 1999; Wilson, 2014). Similarly, the more vascularized grey matter demonstrates greater BH responsivity relative to white matter (Kastrup, Kruger, Glover, & Moseley, 1999; Thomason, Burrows, Gabrieli, & Glover, 2005).

Research Using Breath-hold Hypercapnia Paradigms

Prior fMRI investigations have established the efficacy and utility of BH challenges to generate CVR data providing consistent findings over a range of interesting research questions. Several investigations have examined confounding

breathing effects in task- and resting-state BOLD studies (Abbott et al., 2005; Birn, 2012; Birn et al., 2009; Birn et al., 2008; C. Chang et al., 2008). Other studies used BH tasks to examine hemodynamic response characteristics and ways to improve utilization of BH paradigms (Li et al., 1999; Magon et al., 2009; Stillman et al., 1995; Thomason & Glover, 2008). Good compliance has been established in children (Thomason et al., 2005), across the adult aging spectrum (Handwerker et al., 2007; Kannurpatti et al., 2010; Riecker et al., 2003; Thomason et al., 2005), as well as in individuals with Alzheimer's disease (Silvestrini et al., 2006), CVD (T. Y. Chang et al., 2009; Leoni et al., 2012; H. S. Markus & Harrison, 1992; Silvestrini et al., 2000; Silvestrini et al., 1999; Vernieri et al., 2001), and CVD risk factors (Tchistiakova et al., 2014).

Breath-hold Hypercapnia Studies in CVD

Most BH hypercapnia studies in CVD were conducted in the 90's and early 2000's, predominantly in patients with steno-occlusive disease (T. Y. Chang et al., 2009; Leoni et al., 2012; Silvestrini et al., 2000; Silvestrini et al., 1999; Vernieri et al., 2001). These investigations provided evidence for deficits in CVR as a risk factor for stroke and transient ischemic attacks. Several methods have been used to quantify CVR in response to BH in CVD, including transcranial Doppler ultrasonography and fMRI. Transcranial Doppler ultrasonography measures changes in blood flow velocity in the cerebral arteries and has been the most common method used to quantify CVR in CVD (Leoni et al., 2012; H. S. Markus & Harrison, 1992; Silvestrini et al., 2000; Silvestrini et al., 1999). A BH index (% increase in mean flow velocity during BH/BH duration) can be calculated and used to examine risk for stroke or other cerebrovascular events (Silvestrini et al., 2000; Silvestrini et al., 1999), and to establish cut-off points for

preserved as opposed to impaired CVR in order to distinguish between patients who may benefit most from interventional procedures (H. S. Markus & Harrison, 1992; Silvestrini et al., 1999). Sensitivity of the BH index, which was at least as effective as CO_2 administration, to CVR was demonstrated by a positive relationship with the degree of stenosis in a group of patients undergoing testing for cerebrovascular disease (H. S. Markus & Harrison, 1992). Subsequent normalization of index values among a subgroup of these patients who underwent carotid endarterectomy provided converging evidence. Using the BH index, several studies linked impaired CVR to severity of CVD. Lower index values were the most important predictor of ischemic events in patients with asymptomatic carotid artery stenosis, supplanting baseline characteristics, risk factors, and degree of stenosis (Silvestrini et al., 2000). Moreover, patients with symptomatic occlusion of the middle cerebral arteries had lower BH index values relative to healthy controls and patients with asymptomatic occlusion or stroke without occlusion, and these values were related to severity of ischemic events in the occlusion groups and to greater neurological impairment in symptomatic occlusion group (Silvestrini et al., 1999).

Fewer studies have used BOLD fMRI to estimate CVR in response to BH in CVD. Worse baseline CVR in bilateral middle cerebral artery territories in patients with unilateral carotid stenosis was related to greater increase in cerebral blood flow on the lesion side after surgical treatment (T. Y. Chang et al., 2009). In participants with type 2 diabetes and hypertension, CVR was lower in regions in occipital and parietal lobes, including lingual cortex, cuneus, precuneus, lateral occipital and pericalcarine cortex relative to participants with hypertension only (Tchistiakova et al., 2014). Both,

transcranial Doppler ultrasonography and fMRI studies using CO_2 administration corroborate the BH findings in patients with steno-occlusive disease and cardiovascular risk factors, demonstrating that impaired or exhausted CVR is associated with an increased risk for ipsilateral stroke, transient ischemic attack, and death, and that lower CVR is generally associated with an impaired vascular system (Hamzei et al., 2003; Leoni et al., 2012; Lythgoe, Williams, Cullinane, & Markus, 1999; H. Markus & Cullinane, 2001; Portegies et al., 2014).

The scarcity of BH BOLD fMRI studies in CVD is somewhat surprising. BH paradigms are well established in this patient population and fMRI provides better spatial resolution than transcranial Doppler ultrasonography (Lythgoe et al., 1999). While BOLD BH studies have been more frequent recently and predominantly in healthy participants, their number is still relatively scarce. In addition, CO_2 administration has been favored due to the possibility of quantitative measurements (i.e., control over the amount of CO_2), whereas BH paradigms only yield semi-quantitative measures (e.g., actual length of BH will likely vary from participant to participant) (Fierstra et al., 2013; Mark et al., 2015; Tancredi & Hoge, 2013). In contrast, the many advantages of BH BOLD fMRI, such as participant comfort and ease of setup, in providing CVR information should encourage a routine inclusion to obtain a better understanding of vascular health and to improve BOLD inferences. This is especially important for group comparisons (Samanez-Larkin & D'Esposito, 2008).

Scaling Operations Using Breath-hold Hypercapnia

An important concern in BOLD fMRI studies are confounding vascular contributions which may interfere with the timing and location of neuronal activation,

introducing spatial variability, and limiting interpretation, especially in older adult populations (D'Esposito et al., 2003; D'Esposito et al., 1999; Di, Kannurpatti, Rypma, & Biswal, 2013; Girouard & Iadecola, 2006; Handwerker et al., 2007; Iadecola, 2004; Kannurpatti et al., 2010; Röther et al., 2002). To date, age- and disease-related variations in CVR are generally not addressed methodologically as a source of BOLD artifact in the published fMRI literature on cognitive function in these populations although effective methods have been explored (Biswal, Kannurpatti, & Rypma, 2007; Kannurpatti, Motes, Rypma, & Biswal, 2011b), including studies comparing older adults to younger adults (Handwerker et al., 2007; Kannurpatti et al., 2010). Notably, magnitude differences in the BOLD response to a saccade task in younger vs older adults did not survive cerebrovascular correction in three out of four regions of interest (ROIs), the only difference that remained was observed in primary visual cortex (Handwerker et al., 2007). Moreover, the finding of a greater scaling-induced reduction in BOLD variability during a motor task but not during a cognitive task in older adults relative to younger adults suggests that BOLD variability of the former was of predominantly vascular source while the latter was of predominantly neuronal source (Kannurpatti et al., 2010). Thus, different types of tasks may be differentially influenced by vascular contributions in older as compared to younger adults. Unadjusted observations from these studies would have led to different (and possibly false) interpretations, providing evidence for the importance of addressing cerebrovascular confounds in BOLD fMRI.

Several approaches have used estimates of vasoreactivity derived from BH BOLD as a voxel-wise scaling factor of the task-related BOLD percent signal change (Di

et al., 2013; Gonzales et al., 2014; K. Murphy, Harris, & Wise, 2011; Thomason, Foland, & Glover, 2007). The simplest method divides the task-related BOLD percent signal change by the BH-related BOLD percent signal change in corresponding voxels (Biswal et al., 2007; Handwerker et al., 2007; Kannurpatti & Biswal, 2008; Kannurpatti et al., 2010, 2011b; Wilson, 2014). The result is a relative BOLD percent signal change thought to reflect neuronal activation underlying a given task more accurately. This interpretation assumes that hemodynamic events associated with neuronal activation and BH hypercapnia are similar. Specifically, if task-related BOLD arises from local neuronally initiated hemodynamic events that induce a local increase in oxygenated blood, and BH BOLD arises from global hemodynamic events inducing a global increase in oxygenated blood, their division results in a fractional change that can be interpreted as the task-related signal change with reduced or removed cerebrovascular contributions. In this way, voxel-wise differences in BOLD responsivity stemming from factors other than neuronal events can be corrected.

Scaling studies in healthy younger and older adults frequently report a reduction in BOLD percent signal change, spatial activation extent, and within-and between participant variability as a result of correction for regional differences in CVR (Biswal et al., 2007; Handwerker et al., 2007; Kannurpatti & Biswal, 2008; Kannurpatti et al., 2010, 2011b). Recently, BH scaling has been used to improve localization of brain activation by reducing the effects of vascular factors such as draining veins (Wilson, 2014). Taken together, these studies have provided strong evidence for the utility and efficacy of BH hypercapnia scaling to reduce extraneous cerebrovascular contributions to the BOLD signal across the adult age-range.

Rationale

Age- and disease-related CVR deficits have not been adequately addressed as a potential source of artifact in published fMRI studies in older adult populations. Given the proliferation of fMRI research and an emerging greater understanding of the potential confounding ramifications of vascular factors associated with aging and CVD on the BOLD response, it is essential that effective and simple correction methods be established for routine inclusion in fMRI assessments in these populations. This is especially true for group comparisons employing an “unadjusted” BOLD response (i.e., the typically used BOLD percent signal change), where systematic baseline differences in CVR may produce significant differences in the BOLD percent signal change by way of a disease-related decrease in vascular compliance, rather than neural dysfunction *per se*. The current study appears to be the first to use a CVR correction method, and in particular BH hypercapnia scaling, to address vascular confounds on the BOLD fMRI response in patients with CVD.

Aims and Hypotheses

BH hypercapnia scaling may be an effective cerebrovascular correction method, potentially enabling more valid inferences about brain-behavior relationships investigated with fMRI. The purpose of the current investigation was to examine BH hypercapnia scaling effects in a group of older adults with CVD and a control group, and to determine whether it might be more effective in a patient group with known vascular impairment. The novel application of this approach in this population may be particularly helpful to quantify and potentially remove extraneous BOLD components associated with vascular dysfunction. A basic perceptual VS paradigm was chosen for its relatively

homogenous and robust functional brain response, and in addition, its prior use in older adults with cerebral amyloid angiopathy (Dumas et al., 2012; Peca et al., 2013). All hypotheses were tested in individually defined functional ROIs, where a significant response to VS is observed.

Aim #1: Examine BH hypercapnia scaling outcomes in each group.

Hypotheses: It was predicted that BH hypercapnia scaling will reduce the VS BOLD percent signal change (median percent signal change), its spatial extent (volume of significant response) and variability (coefficient of variation) in each group.

Aim #2: Examine BH hypercapnia scaling outcomes between groups.

Hypotheses: It was predicted that, before scaling, the patient group will demonstrate a VS-associated BOLD percent signal change that is smaller in percent signal change (median percent signal change) and spatial extent (volume of significant response) but more variable (assessed with a test of homogeneity of variance) relative to the control group, and this pattern will persist even after the BH scaling correction, indicative of neural dysfunction associated with CVD. Moreover, it was predicted that BH hypercapnia scaling will result in a greater change in the CVD group relative to the control group (i.e., an interaction).

Aim #3: Examine BH hypercapnia outcomes as an exploratory analysis across the whole brain, both, within and between groups. As scaling has not only demonstrated effects in task-related regions, it has also been useful in reducing artifacts from draining veins and sinuses, and consequently improved localization of brain activation. As CVR

is expected to be more globally impaired in patients with CVD, carrying out a whole-brain analysis may be an effective correction method at a more global level. This is particularly important as prior studies have restricted their examinations to ROIs, and therefore, limited their conclusions.

CHAPTER 2

METHODS

Participants

Complete datasets from 20 cardiac patients and 32 typically aging older control participants were available and constituted the initial pool for this study. Participants in the patient group were diagnosed with CVD (e.g., coronary artery disease, heart attack, and cardiac arrest; none had brain hemorrhage, transient ischemic attack, and stroke) and were recruited from cardiac clinics and hospital services at Rhode Island Hospital, Providence, Rhode Island (USA). Individuals in the control group were recruited from the community using flyers, newspaper and bus ads in the greater Providence metropolitan area. All participants were right-handed, English-speaking, and with normal or corrected vision. Study exclusion criteria were major neurological, psychiatric, or medical (other than CVD in the patient group) disorders known to affect cerebrovascular or brain function, and any contraindication for MRI. Participants in the control group were excluded if they had a history of significant cardiovascular disease (e.g., coronary artery disease or heart failure). All individuals were Caucasian, with the exception of one African-American participant in the patient group and one Asian-American participant in the control group.

Some individuals from both groups were excluded from the participant pool after examination of imaging data. Specifically, three participants in the patient group and two participants in the control group were excluded for anatomical or functional scan

artifacts. For the VS paradigm, one patient and two control participants were excluded due to excessive motion. For the BH task, two patients and six control participants were excluded for excessive motion, and one in each group for noisy data (i.e., >40% of brain volumes were censored as outliers). Participants who provided valid imaging data for both, the VS and BH tasks, were included in the final groups. The final study sample consisted of 14 patients (mean age=70±9, 3 women and 11 men) and 22 typically aging older adults (mean age=61±8, 14 women and 8 men).

All participants provided informed consent prior to study procedures and were given $226 as compensation. The study was approved and monitored by the Institutional Review Boards of Brown University, Rhode Island Hospital, and Butler Hospital in Providence in accordance with the Helsinki Declaration.

Assessment

The data for this study were originally collected over three visits to Brown University, Rhode Island Hospital, and Butler Hospital in Providence. Visit one included an interview and neuropsychological assessment. Visit two included an echocardiogram. All MRI scans were collected at visit three, and included an anatomical and the functional (VS and BH) scans. The data were available for analysis in our laboratory.

Power analysis for paired- and independent-samples *t*-tests were conducted in G*Power 3.1 (Faul, Erdfelder, Lang, & Buchner, 2007), assuming a two-tailed $\alpha<0.05$ and power of 0.80, to provide an estimate of the necessary sample size to detect scaling effects within groups (hypothesis 1) and between groups (hypothesis 2) (Lakens, 2013).

For the paired-sample Student's *t*-tests of scaling outcomes, effect sizes of scaling results were computed from four prior studies of motor and cognitive tasks in younger and older adults (Biswal et al., 2007; Kannurpatti & Biswal, 2008; Kannurpatti, Motes, Rypma, & Biswal, 2011a; Kannurpatti et al., 2011b). The average of these effect sizes was then calculated, which resulted in a Cohen's d_z=2.60, suggesting that a sample size of 14 participants would be more than sufficient to test the proposed within-subject hypotheses.

For the independent-samples *t*-test, effect sizes were calculated using group differences reported between healthy younger and healthy older adults on unscaled and scaled average BOLD percent signal changes during a finger-tapping and a cognitive task (Kannurpatti et al., 2011a). The effect sizes for the unscaled and for the scaled outcomes were averaged across both tasks. The final effect size of Cohen's *d*= 0.40 for the unscaled activation estimates required a total sample size of 200 participants (100 in each group) and the final effect size of Cohen's *d*=0.18 for the scaled estimates required a total sample size of 972 (486 in each group).

Demographics and Clinical Measures: Participants completed a comprehensive battery on health and medication status. Patients provided information on CVD diagnosis.

Image Acquisition: Images were acquired in a single session using a 3 T Siemens TIM Trio scanner (Erlangen, Germany) equipped with a 32 channel head receive array coil. For all MRI scans, head position was stabilized with foam padding. A high-resolution 3D T1-weighted structural brain scan was acquired in the sagittal plane using a magnetization prepared rapid gradient echo (MPRAGE) protocol (repetition time

(TR)=1900 ms, echo time (TE)=2.98 ms, flip angle=9°, field of view (FOV)=256x256 mm, acquisition matrix 256x256, 160 contiguous slices, voxel size=1x1x1 mm). Two functional BOLD scans were conducted using an echoplanar sequence (TR/TE/flip angle=2500 ms/28 ms/90°, FOV=64x64 mm, acquisition matrix 192x192, 42 contiguous axial slices acquired interleaved, voxel size=3x3x3 mm, 96 volumes for the VS and 115 volumes for the BH task). FMRI paradigms were presented using E-prime (Psychology Software Tools, Sharpsburg, USA) and back-projected onto a screen visible to the participant via a mirror mounted to the head coil.

Visual Stimulation: A passive VS paradigm known to reliably activate visual cortex was presented in a blocked design, alternating six 20 seconds blocks of a flickering checkerboard with six 20 seconds blocks of crosshair fixation. The checkerboard stimulus comprised of a 6x6 matrix of black and white squares. A flickering state was generated with a temporal square wave alternating black and white squares with a period of 100 msec (equivalent to 10 Hz). Participants were instructed to either fixate on the center of the checkerboard or on a white crosshair against a black background.

Breath-hold Hypercapnia: A BH paradigm was used to induce a global hypercapnia-based vascular response. High correspondence between CO_2 administration and BH hypercapnia induction on various parameters, including BOLD intensities (Biswal et al., 2007; Kannurpatti & Biswal, 2008; Kastrup, Kruger, Neumann-Haefelin, & Moseley, 2001), have provided evidence for similar capacity of BH to probe CVR in fMRI studies (Tancredi & Hoge, 2013). In addition to their demonstrated effectiveness, advantages of BH challenges include their simplicity in task demand,

minimal set-up time, and robustness in eliciting a reproducible BOLD response (Magon et al., 2009). Unlike CO_2 inhalation, which involves either a mouthpiece or tight-fitting mask for gas mixtures delivery, BH tasks do not require additional equipment and cost, and are a safe and easier to perform alternative, especially suitable in older adult and patient populations (Fierstra et al., 2013; Kastrup et al., 2001; H. S. Markus & Harrison, 1992). The paradigm used in the present study consisted of six 15 seconds blocks of breath-holding alternating with six 30 seconds blocks of self-paced breathing. Prior research has shown good detectability (Liu et al., 2002) and reproducibility (Magon et al., 2009) of BH blocks 15 seconds. To avoid movement associated with breath-holding, a countdown of “3”, “2”, “1” (1 second each) was displayed prior to the start of BH blocks, signaling to the participants that the BH block was about to begin. Participants were trained to perform the task before entering the scanner using a standardized procedure in which they were instructed to calmly transition from self-paced breathing to holding their breath without moving their head or body.

Functional Data Analysis

Preprocessing, individual-level, and group-level whole-brain analyses were carried out using Analysis of Functional Neuroimages (AFNI) (Cox, 1996).

Preprocessing

Preprocessing of both functional runs was identical and included slice-time correction and affine registration of each volume to the third volume to correct for head movement. Data of participants with head movement of >3.0 mm (one voxel size) in any direction were omitted from analyses. The individual’s anatomical image was first aligned to the volume-registered functional run, skull-stripped, and then normalized into

Talairach space based on a publicly available template (TT_N27; offered in AFNI). The functional runs in native space were then aligned to the anatomical image in Talairach space using the concatenated transformation matrices from the volume registration, anatomical to functional alignment, and anatomical transformation into standard space steps (this concatenated file was used also to align grey matter masks in the functional ROI generation described below). A 4-mm full-width at half-maximum Gaussian spatial filter was applied to the time series. Furthermore, the BOLD signal was scaled by dividing every time point of the smoothed time series by its mean. The resulting signal represents a relative magnitude change and facilitates the comparison across participants as the acquired data from the scanner have no intrinsic physiological meaning and can differ substantially between brain regions and participants. The relative time series is then converted to a percent change by multiplication with 100 and permits interpretation of the β estimates as percent signal change from baseline.

Individual-level Analyses

At the individual level, the general linear model was applied to the BOLD signal in each voxel. For the VS paradigm, a prototypical hemodynamic response function was generated by convolving the timing of the checkerboard blocks with an incomplete gamma function ("BLOCK" model in AFNI). For the BH task, the timing of the 3 seconds countdown prior to each BH block was convolved using the same BLOCK model. In contrast, the delayed onset and sluggish trajectory of the BH BOLD response (Biswal et al., 2007; Leoni et al., 2008; Liu et al., 2002) was estimated using a deconvolution approach with a series of 7 piecewise linear B-spline basis functions ("TENT" model in AFNI) over a time window of 30 seconds, with each tent covering an interval of 2 TRs

(equivalent to 5 seconds). This approach yielded 7 separate amplitudes at consecutive time points with the first amplitude estimated 12 seconds after begin of the BH block and the last amplitude estimated 42 seconds after begin of the BH block; each amplitude is associated with a β coefficient and corresponding *t*-statistic. The magnitude of each was interpreted as percent signal change from baseline. The hemodynamic response models for each paradigm were then entered into two otherwise identical generalized least-squares regression models which included regressors of no interest for motion (translation and rotation in three planes) and linear, quadratic, and cubic drift. TRs with average motion >0.4 mm/TR were censored. Temporal autocorrelation in the residuals was estimated with an autoregressive moving average model (1,1) using restricted maximum likelihood.

Individual activation maps for VS were thresholded at $p<.01$ for functional ROI volumes described below (cluster family-wise error corrected (cFWE) at $\alpha<.01$; all imaging thresholds are voxel-wise, nearest-neighbors touching face, corner, and edge, and take inherent and applied spatial correlation of the data into account).

Group-level Analyses

For each group, overall patterns of brain activation to both paradigms were examined with two one-sample mixed-effects analyses (Chen, Saad, Nath, Beauchamp, & Cox, 2012) to obtain summary maps for validation of expected activation patterns. The β maps for the VS vs fixation contrast were thresholded at $p<.01$ (cFWE at $\alpha<.01$ with a minimum cluster size of 40 voxels). This threshold was chosen as brain activation to VS is robust. The β maps for the BH vs self-paced breathing contrasts were thresholded at a more stringent $p<.001$ as the BOLD response to BH is global and

robust, swamping interesting details (minimum cluster size=13 voxels). Seven β maps were available (i.e., seven tents providing an amplitude at seven consecutive time points spaced 5 seconds apart) for each individual participant to contribute to the group BH summary activation map. There are several ways to construct a summary group map, for example, by taking the average across the seven amplitudes or by selecting only one specific time point (i.e., a specific amplitude). A "peak" β map was defined for each participant, namely the map with the largest average β coefficient in the individual's functional ROI described below. This "peak" β map was used in all analyses involving BH data.

Between-group differences in brain response to VS were examined with a whole-brain independent-sample mixed-effects analysis. This comparison was carried out to obtain baseline clusters of significant group differences in visual cortex in which scaling effects can be further investigated. The resulting β-map was thresholded at $p<.05$ (cFWE at $\alpha<.05$, minimum cluster size=124 voxels). To examine potential motion artifacts, group differences in average motion/TR, maximum motion displacement, and censored TRs were investigated with independent-samples Student's *t*-test set at $p<.05$.

Individual Regions of Interest

To test hypotheses in visual regions more accurately, potential biases of voxels that are unresponsive to VS or those of partial volume effects were minimized by generating individual functional ROIs formed by the intersection of: a) voxels of significant positive association with VS in the individual activation maps (described above) and b) voxels at least 60% likely to comprise grey matter. To accomplish this, segmented T1-weighted images (SPM12b; Wellcome Trust Centre for Neuroimaging,

London, United Kingdom) in native space were transformed into Talairach space using the individual's transformation matrix from the various normalization steps described in the preprocessing section above, and aligned to the grid of the individual's VS *β*-map (final voxel size 3x3x3mm).

Scaling of Visual Stimulation Activation

Scaling Manipulation

Hemodynamic scaling was performed at two levels: in functional ROIs and across the whole brain, and carried out by dividing the VS-related BOLD percent signal change with the normalized BH BOLD percent signal change in corresponding voxels. The BH percent signal change was normalized in each voxel by division with the median BH percent signal change in the volume under investigation (i.e., the median BH percent signal change in functional ROIs or across the whole brain) to account for regional heterogeneity in the range of BH values while preserving cerebrovascular information at the voxel level. The scaled result can be interpreted as the BOLD amplitude to VS normalized for vascular variability.

Hypothesis Testing in Functional ROIs

The median BOLD percent signal changes in functional ROIs were normally distributed and variances were homogeneous (tested with Shapiro-Wilk and F-tests, respectively), indicating the use of parametric statistics (Figure 3).

The hypothesis that scaling reduced the effects of cerebrovascular confounds, thereby reducing the VS BOLD response, was tested on the median percent signal change in individual's functional ROIs using a paired-sample Student's *t*-test in each group. Changes in activation extent pre-to-post scaling were quantified by counting

voxels with VS percent signal change corresponding to $p<.05$ in individual ROIs. To test the hypothesis that scaling reduced VS BOLD signal variability, coefficients of variation (CV) were defined as the standard deviation divided by the mean, and fractional changes in the variability from pre-to-post scaling were calculated by subtracting 1 from the ratio of CV of the scaled percent signal change to the CV of the unscaled percent signal change and multiplying the result by 100.

The hypothesis that the groups differ on the scaled VS BOLD percent signal change was tested with an independent-samples Student's *t*-test. Voxel counts as described above will be used to compare activation extents between groups. A group by treatment mixed-factorial analysis of variance was used to examine potential differential scaling effects (i.e., an interaction). The hypothesis that scaling reduces variability to a greater degree in the CVD group was examined with fractional changes in the CV of the VS BOLD percent signal changes from pre-to-post scaling.

Exploratory Whole-brain Scaling

The whole-brain data included large outliers (predominantly located in drop-out regions, e.g., orbitofrontal cortex) in the BH and VS brain activation estimates, which produced highly-skewed, non-normal distributions. Transformations, such as the natural logarithm, have been used to make highly skewed distributions more normal. This approach (as well as others, e.g., square root or inverse transformations) was not readily useable due to negative values, occasional zeros, and positive values less than 1 that are part of the dataset. In such circumstances, a constant can be added to obtain only positive numbers before carrying out the log transformation. However, the outlying values in the current study greatly differ between paradigms and from one participant to

the next, and are generally very large (for examples see Table 2). Adding such large constants is not advised and could considerably affect the *p*-values of the group statistic (Changyong et al., 2014). As the logarithm data transformation technique was not applicable to reduce skew in the distributions, non-parametric tests were used.

Non-parametric methods, such as Wilcoxon signed-rank and Wilcoxon-Mann-Whitney rank-sum tests, do not require the data to be normally distributed and are robust in the presence of outliers. We used these two median-based tests as non-parametric counterparts to paired-sample and independent-sample Student's *t*-tests at the whole-brain level, respectively. The median absolute deviation (MAD), instead of standard deviation, was used a non-parametric measure of variability.

The effectiveness of whole-brain scaling to reduce confounding cerebrovascular contributions to the BOLD signal was explored within each group using a voxel-wise Wilcoxon signed-rank test. Between-group differences in the scaled BOLD percent signal change were examined using a voxel-wise Wilcoxon-Mann-Whitney rank sum test. To investigate whether scaling affected the groups differently (i.e., an interaction), difference scores of the VS BOLD percent signal change pre- minus post-scaling were calculated and a Wilcoxon-Mann-Whitney rank-sum test employed to test for differential group effects. All maps were thresholded at $p<.05$ (cFWE at $\alpha<.05$, cluster extent=124 voxels). A count of voxels with a) median and b) MAD≥0.50 of the pre-as well as the post-scaling group maps was obtained as a measure of change in activation extent and variability.

In addition, groups were compared on visual acuity (left and right eye) with Student's *t*-tests and $p<.05$ was required for significance to exclude brain activation confounds that are due to visual dysfunction (i.e., not disease-related sources).

All statistical analyses are two-tailed and were carried out in R (Team, 2014) (except preprocessing, individual-level, and group-level whole-brain analyses, which were carried out using AFNI).

CHAPTER 3

RESULTS

A summary of sample characteristics is provided in Table 1. Fourteen participants (8 women and 6 men) were drawn from the larger control cohort and age-matched to the patient group (3 women and 11 men). As intended, the matched groups did not significantly differ in age (independent-samples Student's $t(26)=-1.12$, $p=.27$). They also did not significantly differ in gender composition (3 women in the patient group and 8 women in the matched control group; Pearson's $\chi^2(1)=1.58$, $p=.21$). The results discussed below relate to the patient and matched control group. Findings from the larger control group cohort will be discussed separately at the end of this section.

Paradigm Results

Visual Stimulation

The whole-brain voxel-wise contrast of VS versus fixation revealed expected patterns of brain activation and deactivation in each group (Figure 1, top two rows). Activation patterns included bilateral primary visual cortex and regions in occipitoparietal and occipitotemporal cortices that are associated with higher-order visual processing (Kwong et al., 1992; Zeki et al., 1991). Relative task-induced deactivation that is consistent with resting state networks was observed in posterior cingulate cortex, precuneus, bilateral inferior parietal lobule, and bilateral medial and superior frontal gyri (Biswal, Yetkin, Haughton, & Hyde, 1995; Raichle et al., 2001)

Breath-hold Hypercapnia

In response to BH relative to self-paced breathing, both groups exhibited a robust global rise in BOLD signal intensities primarily in grey matter (Figure 1, top two rows) (Kastrup, Kruger, Glover, & Moseley, 1999; Kastrup, Kruger, Glover, Neumann-Haefelin, et al., 1999; Riecker et al., 2003; Stillman et al., 1995). Preparing to hold one's breath (e.g., taking a deep breath prior to holding it), may lead to task-correlated motion. To examine whether head motion contributed to BH after correction at the individual level, correlations between BH BOLD estimates and each, average head motion per TR and absolute head motion displacement, were examined. Non-significant results were observed in each group (all $p>.20$). Averaged BH BOLD time courses and the hemodynamic response model in individual functional ROIs that were defined by significant positive VS effects (i.e., in regions where scaling hypotheses were tested) and across the whole-brain are displayed in Figure 2.

Scaling Results

Hypothesis Testing in Functional Grey Matter ROIs

The average median BOLD percent signal changes of BH, unscaled, and scaled VS in ROIs were normally distributed (Wilk-Shapiro tests; $p>.43$ for all three in the patient group and $p>.15$ in the matched control group with the exception of $p>.07$ for the BH percent changes). Between groups, the variances of the average median unscaled and scaled VS intensities did not significantly differ (F-tests; both $p>.14$). Thus, parametric statistical analyses were used.

Individually determined functional ROIs defined by significant positive response during the VS paradigm varied considerably in size (Table 1). To provide support for

CVR contributions to the task-related hemodynamic response, Pearson's correlations between BH and the unscaled VS BOLD percent signal changes were computed in functional ROIs (Table 1). On average, the two paradigms showed a relatively strong positive relationship in the patient group (Pearson's r=0.45±0.27) as well as in the matched control group (Pearson's r=0.50±0.20), with BH estimates accounting for 27±18% of the variance in the task BOLD amplitudes in the patient group and for 28±18% in the matched control group (simple linear regressions calculated separately for each participant; all correlations and regressions were statistically significant at p<.001).

VS response pre and post scaling is depicted in Table 1 along with BH responses. Figure 3 shows boxplots of their distribution before and after scaling in each group. As hypothesized, the average median VS percent signal change was significantly (t(13)=2.76, p=.02) reduced from 1.17±0.23 to 0.94±0.34 in the patient group and significantly (t(13)=4.13, p=.01) reduced from 1.05±0.21 to 0.95±0.22 in the control group (see Table 1). A reversal of the positive relationship between BH and the unscaled VS magnitudes provided converging support; in the patient group, an average Spearman's rho=-0.27±0.35 was observed compared to an average rho=-0.34±0.19 in the matched control group.

Differences in the extent of activation from pre-to-post scaling could not be quantified due to spuriously high percent signal changes that resulted from division with small BH values (Table 2). These magnitudes varied greatly across participants and considerably skewed the distributions, and as such, a uniform decision rule on what constitutes an outlier could not be devised. In contrast to our hypotheses, these high

magnitudes also resulted in greater variability after scaling. In the patient group, the CV increased from 0.20 to 0.36 and from 0.20 to 0.23 in the control group, amounting to a fractional increase of 80% in BOLD variability among participants in the patient group and 15% increase among participants in the control group.

Between groups, there were no significant differences in the size of the functional ROIs (Student's $t(26)=0.85$, $p=.40$) or in the VS intensity before (Student's $t(26)=-1.32$, $p=.20$) or after (Student's $t(26)=-0.08$, $p=.94$) scaling. There was no significant group by scaling interaction ($F(1, 26)=1.43$, $p=.24$). The groups also did not differ in variance either before (F-test$(13, 13)=0.86$, $p=.79$) nor after (F-test $(13, 13)=0.43$, $p=.14$) scaling. In addition, the BH effect used for scaling did not differ between groups (Student's $t(26)=0.47$, $p=.64$) These findings indicate that there were no group differences before or after scaling in brain activation in functional ROIs and that scaling had no differential effect by group in these regions.

Exploratory Whole-brain Results

Within-group Effects

The patterns of scaling effects were very similar in each group. The VS BOLD percent signal change significantly decreased with scaling in primary and secondary visual areas relative to the unscaled BOLD percent signal change in each group (Figures 5 and 6, Table 3). Moreover, significantly attenuated negative percent signal change was observed in regions associated with resting state networks. These include the default mode network, comprising precuneus, inferior and superior parietal lobule, cingulate cortex and medial frontal gyri, and sensory network in right temporal cortex. The clusters of significant scaling effects tended to overlap with sinuses (e.g., straight,

inferior and superior sagittal, occipital, and confluence of sinuses) and vasculature (e.g., anterior, middle, and posterior cerebral arteries) (Di et al., 2013; Yuan et al., 2013).

Scaling also reduced activation magnitude and variability in both groups as indicated by a decrease in the overall range (i.e., all brain voxels) of the VS BOLD percent signal changes and their MADs (Figure 7). In the patient group, the median VS percent signal changes originally spanned values from -1.6–2.8 before scaling which decreased to -0.4–1.1 after scaling and the range of the MAD reduced from 0–3.7 before to 0–1.1 after scaling. Similarly, the range of median VS percent signal changes declined from -1.7–2.5 before to -0.5–1.6 after scaling in the matched control group and the MADs reduced from 0–4.5 to 0–1.3.

Scaling reduced activation extent and variability in both groups when counting voxels at an arbitrary threshold of median BOLD percent signal change≥0.50 (Figure 7). In the patient group, there were 1672 voxels with median VS percent signal change≥0.50 counted before scaling and 206 voxels counted after scaling (note that these counts only include activated voxels as deactivation magnitudes were much smaller than 0.50), and 3346 voxels with MAD≥0.50 were counted before scaling vs 136 after scaling. Similar results were observed in the matched control group, where 1474 voxels of median VS percent signal change≥0.50 passed before vs 619 after scaling, and the number of voxels with MAD≥0.5 reduced from 3006 to 409. Almost all voxels with MAD≥0.5 were clustered in visual regions or areas prone to noise (e.g., signal-dropout in orbitofrontal cortex and sinuses), which disappeared with scaling. While scaling reduced the number of voxels with MAD≥0.5, it increased the magnitude of those remaining (note, however, that these values do not exceed MAD above 1.3 and

1.1 in the patient and matched control group, respectively). Overall, the reduction in activation extent and variability resulted in more homogenous activation patterns with improved localization to task-related grey matter regions, providing support for using BH scaling as an effective correction method across the whole brain.

Between-group Effects

The whole-brain group comparison of VS BOLD percent signal change before scaling, revealed that the patient and the matched control groups significantly differed in only one cluster (143 voxels; center of mass in Talairach space: x=-2, y=-23, z=+25) comprising portions of right anterior cingulate and superior frontal gyri (image not shown). No area in visual cortex demonstrated significant group differences. After scaling, groups significantly differed in a cluster (127 voxels; center of mass in Talairach space: x=+17, y=+88, z=+15) in left middle occipital gyrus, extending into cuneus and Brodmann Area 18, where the patient group displayed a smaller median scaled VS percent signal change of 0.12±0.22 relative to the matched control group with 0.56±0.34 (see Figure 8).

A post-hoc group by scaling mixed-factorial analysis of variance was used to further examine the median BOLD percent signal change in this cluster. There was a trend-level significance ($F(1, 26)=3.31$, $p=.08$) for the interaction and significant main effects for scaling ($F(1, 26)=12.02$, $p=.01$) and for group ($F(1, 26)=10.15$, p=.01). Following up with paired-sample Student's *t*-tests, the patient group demonstrated a significant ($t(13)=3.14$, $p=0.01$) reduction in the average median BOLD percent signal change, which was not seen in the matched control group ($t(13)=1.53$, $p=0.15$). In addition, an independent-sample Student's *t*-test showed a trend-level significance

($t(26)=1.90$, $p=.07$) for a group difference in the average median unscaled BOLD percent signal change of 0.40±0.35 in the patient group compared to 0.65±0.35 in the matched control group. These results suggest that the patient group displayed a smaller median VS BOLD response that was reduced to a greater extent relative to the matched control group.

When compared on the whole-brain voxel-wise pre-minus-post scaling difference scores, there were no significant differences between the groups, and as such, there does not appear to be a group by scaling interaction at the whole-brain level. In addition, for both, visual stimulation and BH paradigms, there were no significant group differences in average head motion per TR, absolute head motion displacement, and number of censored TRs (all $p>.30$).

Results in Larger Control Group Cohort

Generally, results from the larger control group cohort were very similar to those observed in the matched groups, both in functional ROIs and on the whole brain (Figures 5 and 6, Table 3).

At the functional ROI level, activation volumes ranged from 115 to 2851 (1441±744), with an average median BH BOLD signal percent signal change of 0.90±0.42 and a significant (Student's $t(21)=4.29$, $p=.01$) reduction of VS percent signal change from 1.14±0.24 to 1.01±0.22. The CV changed from 0.21 to 0.22, which translates into a fractional increase of 5% in BOLD variability among participants. On the whole brain, scaling results mirrored those of the other groups (Figures 5 & 6, Table 3).

The overall range of VS percent signal change decreased from -1.35–2.77 before to -0.43–1.30 after scaling and the number of voxels with median percent signal change≥0.5 was reduced from 1406 to 618. The overall MAD range decreased from 0-3.5 to 0-0.9 and 222 voxels surpassed MAD≥0.5 after scaling while 2774 did so before, with the remaining voxels being similarly distributed like the other two groups (Figure 7). These findings suggest that the observed scaling patterns are robust and that the results in the smaller groups may have sufficient power, and therefore, are promising for future investigations using this correction method.

CHAPTER 4

DISCUSSION

The primary goals of the current study were to utilize BH hypercapnia scaling of the BOLD response to VS in order to control for individual differences in cerebral vasoactive capacity in a group of older adults, and to determine whether scaling may be a particularly effective method in a patient population with known vascular impairment. As hypothesized and consistent with prior literature, BH hypercapnia scaling decreased the magnitude of brain activation estimates in regions associated with VS (Biswal et al., 2007; Handwerker et al., 2007; Kannurpatti & Biswal, 2008; Kannurpatti et al., 2010, 2011b). The predictions about the diminishing effects on spatial extent and variability were not supported in these regions, and the predicted differential benefit in the patient sample received only limited support. However, whole-brain, voxel-wise analyses suggested that scaling may reduce variability and extent of activation on a global level. Results from this study indicate that a simple BH hypercapnia challenge can be used as an effective method to correct age-and disease-related CVR confounds to the task-related hemodynamic response in older adult populations.

Validity and Integration with prior Visual Stimulation and Breath-hold Hypercapnia Literature

Passive viewing of a flickering checkerboard elicited expected activation in each group in regions previously associated with the processing of visual information, including primary and higher-order visual cortices in occipital, temporal, and parietal

lobes (Kwong et al., 1992; Zeki et al., 1991). Relative deactivation occurred in regions associated with resting state networks, particularly the default network, which has been previously reported to deactivate in response to similar VS paradigms (Biswal et al., 2007; Raichle et al., 2001).

In functional ROIs, which were individually defined based upon the positive brain response to VS, patients displayed an average median BOLD percent signal change of 1.14 whereas controls exhibited an average median percent signal change of 1.06. Both of these observations fall well within the range reported by other VS studies (between 0.57 and 4.20 percent signal change) with flickering checkerboards (Ances et al., 2009; Buckner et al., 2000; Donahue et al., 2009; Gati et al., 1997; Kastrup, Kruger, Glover, & Moseley, 1999), including samples of older adults with CVD (Dumas et al., 2012; Peca et al., 2013). Specifically, older adults with cerebral amyloid angiopathy demonstrated an average BOLD amplitude of 0.65 compared to 0.89 reported for healthy older adults during 20 seconds blocks of a flickering checkerboard (Dumas et al., 2012). In another study in this population, an average signal change of 2.57 was observed in patients compared to 3.57 in the control group in response to 40 seconds of VS (Peca et al., 2013). Therefore, the activation amplitudes observed in patients in the current study during 20 seconds stimulus presentation blocks fall in the expected range based on prior studies in a related population using equal or longer stimulus durations.

The BH challenge elicited a characteristic global BOLD response that was detected primarily in grey matter (Gati et al., 1997; Kastrup, Kruger, Glover, & Moseley, 1999; Kastrup, Kruger, Glover, Neumann-Haefelin, et al., 1999; Riecker et al., 2003; Stillman et al., 1995). The average median BH percent signal change estimates in

functional ROIs were also consistent with prior literature, amounting to 0.74 in the patient group and 0.82 in the matched control group (Leoni et al., 2008; Magon et al., 2009). Although the BH BOLD percent signal change varies widely across studies, with estimates as low as 0.43 up to 12.7 (Birn et al., 2008; Magon et al., 2009; Riecker et al., 2003), BH blocks of 15 seconds have been reported to produce a hemodynamic response amplitude between 0.8 and 2.1 (Leoni et al., 2008; Liu et al., 2002; Magon et al., 2009). Observations in the current study, therefore, fall within the range expected from previous findings.

The shape and timing of the BOLD response to BH hypercapnia also replicated prior literature (Handwerker et al., 2007; Leoni et al., 2008; Magon et al., 2009). A tri-phasic time course is typically seen after inspiration, with an initial small increase followed by a decrease below zero and another large increase above zero with an extended descent back to baseline, and sometimes an undershoot (see Figure 4 for comparison with Figure 2). Onset times between 14 to 16 seconds, time-to-peak between 13 to 31 seconds, and time to the first half of the full-width-half-maximum between 16 and 21 seconds for BH blocks of 15 seconds duration have been reported, depending on the definition used to quantify these hemodynamic characteristics and the brain region under investigation (Leoni et al., 2008; Liu et al., 2002; Magon et al., 2009). The time it took the BH BOLD signal to return to baseline after the start of the BH block was not explicitly stated in these studies but appears to fall roughly between 40 to 50 seconds (Figure 4) (Leoni et al., 2008; Magon et al., 2009). In older adults, the response also extends up to 50 seconds; however, stimulation duration was double of that in the present study (Riecker et al., 2003).

Such a prolonged period for the BH hypercapnia response may induce overlap between the BOLD responses from one block to the next, artificially increasing the subsequent magnitude, if the interval of normal breathing in between is too short. This is unlikely to represent a confounding factor in this study. The design employed here consists of 15 second BH blocks followed by 30 second blocks of self-paced breathing, summing to 45 seconds after start of the BH block, or 48 seconds if including the 3 seconds of instructions. Furthermore, based on prior literature it is expected that shorter breath-holds result in a shorter BOLD response (Leoni et al., 2008; Liu et al., 2002; Magon et al., 2009). Accordingly, the timing of our study design should theoretically allow for the signal to return to baseline before onset of the next block. Indeed, BH BOLD reactivity in the present study exhibited a return to baseline before the next BH block started, indicating that the hemodynamic responses did not overlap (Figure 2). The delayed onset of the BOLD response provides an additional temporal buffer, particularly since the response is modeled beginning 12 seconds after the start of the BH block, when residual influences should be absent.

Tests of the Hypotheses

Hypothesis-testing in functional ROIs yielded mixed results. Consistent with our predictions, a significant post-scaling reduction in the activation magnitude was observed in each group. However, spuriously high values skewed the distribution and precluded voxel counts, and consequently, the comparison of brain activation extent before and after scaling. Excluding voxels with outlying scaled percent signal changes was not a fitting approach as a uniform decision rule could not be applied across participants. For example, choosing an arbitrary threshold of removing values>2 MADs

(standard deviations cannot be used due to these outliers; see Table 2) would have likely biased the results as similar, physiologically plausible values that were just above this threshold would have been excluded. A potentially successful approach to obtain voxel counts for extent comparisons may be to examine a proportion of values of the total number of values in a given functional ROI. For example, the number of values in this proportion centered around zero that are above some cut-off could be calculated pre- and post-scaling. Zero as the center would seem a better choice as opposed to the median for example, given that activation estimates that are physiologically meaningful in this range are expected to decrease with scaling (i.e., become closer to zero), and the outliers are much greater than zero. Furthermore, these high values caused an increase in the variability of the scaled BOLD percent signal, which negated a decrease after scaling as was expected. Between groups, there were no significant differences in the VS BOLD percent signal change or its variability before or after scaling, and no interaction took place. Again, the groups could not be compared on changes in spatial activation extent due to the high values after scaling.

The lack of expected findings can be partially attributed to the variability in the BH BOLD data. The CVs were at the higher end of the spectrum seen in the literature, especially in the patient group (0.62 vs 0.50 in the matched control group), although similar values have been reported for BH blocks of 9 seconds (0.56) (Magon et al., 2009), 14 seconds (0.50) (Donahue et al., 2009), and 18 seconds (0.48) (Thomason et al., 2007). While the VS BOLD percent signal change decreased to a greater degree in the patient group relative to the control group in the present study, the inter-subject variability may have impeded the detection of group differences and differential scaling

effects. Overall, between-group results in functional ROIs do not support the hypothesis that BH hypercapnia scaling was more beneficial in the patient group relative to the matched control group. Ultimately, while the variability in the BH BOLD estimates appears to have decreased the effectiveness of the scaling operation in functional ROIs, particularly for the patient group, and possibly lead to underlying group differences going undetected, the significant decrease in the VS BOLD percent signal change is consistent with the literature and an encouraging finding.

Another possible explanation for the current findings may be related to the generation of the functional ROI masks. The stringent threshold of $p<.01$ at $\alpha<.01$ and voxels having to touch faces, corners, and edges to form clusters may have restricted the range of activation intensity, and thus the regions examined were restricted to the most active in both groups. Future studies should consider using a more lenient thresholding procedure.

Power analyses using effect sizes from prior studies suggested sample sizes of more than 100 participants per group to detect between-group differences. However, these were drawn from a study using a different design than the current one, which was carried out between healthy younger and older adults (Kannurpatti et al., 2011a), where age effects may be smaller than disease-related effects. Future investigations are needed to illuminate scaling outcomes that are due to age- versus disease.

The unscaled VS and BH percent signal changes in functional ROIs were, on average, relatively strongly positivity correlated in each group and the magnitude of the hemodynamic response to hypercapnia can predict the magnitude associated with neuronal task activation. Since the paradigms were independent and the BOLD

response to BH is global (i.e., not showing effects specific to those regions engaged by passive viewing of the flickering checkerboard), their correspondence should be due to vascular sources as opposed to neural sources. Scaling, therefore, should result in brain activation estimates that are corrected for variations in CVR. Indeed, correlations between BH and the scaled VS estimates are all negative (except for three participants in the patient group and one participant in the matched control group), indicating that the normalized percent signal change is greatest when vascular contributions are lowest and vice versa.

Whole-brain Scaling

Whole-brain scaling was explored as a global CVR correction method to improve BOLD signal validity and to potentially detect brain regions sensitive to vascular artifacts. At the whole-brain level, significant pre-to-post scaling differences were observed in activated and de-activated task-related regions when compared to the baseline group activation maps (Figure 1). In activated regions, the percent signal change was reduced and became less negative in deactivated regions. These patterns were observed in each group and suggest that confounding variations in the vasodilatory capacity have been minimized (Biswal et al., 2007; Di et al., 2013; Handwerker et al., 2007; Kannurpatti & Biswal, 2008; Kannurpatti et al., 2010, 2011a, 2011b). Converging with the present findings, there is evidence that local cerebrovascular contributions act to amplify the BOLD amplitude in both directions – positive (activated) as well as negative (deactivated) – relative to rest (Di et al., 2013; Yuan et al., 2013). This means that voxels with greater sensitivity to vascular influences exhibited greater positive activation but also greater negative activation. Prior studies

have shown large positive correlations between BH activations and the amplitude of low-frequency fluctuation derived from resting-state scans across the whole brain (Di et al., 2013), and furthermore have used the latter as a vascular scaling factor for task-related BOLD percent signal changes similarly to using BH BOLD percent signal changes (Di et al., 2013; Kannurpatti & Biswal, 2008; Kannurpatti et al., 2011a, 2011b; Yuan et al., 2013), showing that both are comparably effective, including in older adults (Kannurpatti et al., 2011a). Similarly, lower connectivity in resting-state networks and decreased working memory activation were identified after using BH delay information to correct for variations in vascular latency (C. Chang et al., 2008). As such, the significantly attenuated signal observed in resting state regions after scaling in this study may indicate diminished vascular influences, or conversely, point towards their sizeable influence. The effects of scaling to mitigate regional sensitivity of the task-related BOLD signal to vasoactive contributions in task-positive as well as task-negative brain networks highlight the importance of normalizing CVR in older adult populations. The apparent vasoactive influence has also been observed in task-negative regions is in line with a recent increase in attention focused on examining the vascular contributions to resting-state activation patterns, indicating that these neurophysiological interrelationships are understudied. This is of particular concern as resting-state paradigms have become a popular method to investigate brain function and mapping of networks in older adult populations (Ferreira & Busatto, 2013; Mark et al., 2015).

Another finding of the present study relates to the utility of BH scaling to suppress large activation magnitudes in voxels with greater vascular contributions located in regions of vascular density, sinuses, draining veins, and large vessels (C.

Chang et al., 2008; Di et al., 2013; Stillman et al., 1995; Wilson, 2014). For example, an average percent signal change of 3.3±0.2 was reported for VS in grey matter compared to 15.1±1.2 in draining veins in primary visual cortex at 4T (Gati et al., 1997). As would be expected from a cerebrovascular normalization method, post-scaling suppression of the BOLD percent signal change in the current study tended to coincide with voxels in these regions. These prominently include the border between occipital cortex and the cerebellum (transverse, straight, and confluence of sinuses) and cingulate cortex (inferior sagittal sinus). Also included are vessels, such as the middle and posterior cerebral arteries in the Sylvian fissure, observable in the patient map in Figure 5. As a result, activation extents were reduced as intensities in voxels with higher blood content were diminished or eliminated, and activation patterns appear more localized to grey matter (Di et al., 2013; Wilson, 2014). This scaling outcome may be particularly beneficial in older adults who present with atrophy where the increased space between gyri is more likely to contain false positive activation peaks.

Whole-brain between-group voxel-wise contrasts of the scaled VS BOLD percent signal change revealed a cluster of significantly lower brain activation in visual cortex in the patient group relative to the control group. Prior studies have reported a smaller BOLD amplitude in visual cortex during a checkerboard paradigm in older adults with cerebral amyloid angiopathy relative to healthy older adults (Peca et al., 2013), and this may be due to impaired CVR as the absolute baseline blood flow in visual cortex was similar between groups (Dumas et al., 2012). Thus, the present finding may reflect true differences in neural activity that can be attributed to effects of CVD, which were only identified after removal of disease-related alterations in cerebral vasoreactivity, since

our groups were matched on age and had similar visual acuity. A prior study reported significantly lower CVR (quantified with a BH paradigm almost identical to the one used in the current study) in occipital and parietal cortices and cortical thinning in lingual and fusiform gyri in participants with hypertension and type 2 diabetes relative to participants with hypertension alone (Tchistiakova et al., 2014). In the present study, both groups contained participants with hypertension and diabetes, although roughly twice as many participants the patient group exhibited these CVD risk-factors. Assuming the individual CVR measure applied as a hypercapnia scaling factor can correct for idiosyncratic impairments in vasoreactivity associated with CVD and risk factors, significant between-group differences would have a neural source.

Alternatively, disease-related white matter damage may underlie the findings of significant post-scaling differences. In a prior study, lower BOLD amplitude in visual cortex in patients with cerebral amyloid angiopathy was significantly related to white matter lesion volume and number of microbleeds (Peca et al., 2013). Similarly, longer time to peak of the BOLD signal in visual cortex was significantly linked to the volume of white matter hyperintensities (Dumas et al., 2012). In contrast, white matter hyperintensities did not account for significant group differences in CVR and cortical thinning between individuals with hypertension and type 2 diabetes relative to those with hypertension alone (Tchistiakova et al., 2014). Measures of structural damage would provide further information and are suggested for future studies.

Limitations

While these results are compelling, there are important limitations. First, BH hypercapnia does not provide controlled dosing of CO_2 which may have contributed to

the variability observed in the BH BOLD response (Fierstra et al., 2013). Individual differences in task performance, such as holding one's breath for precisely the required block length, variations in breathing rate and depth during self-paced breathing, inspiration extent prior to breath-holding, and lung capacity are known to affect the accuracy of BH estimates (Fierstra et al., 2013; Thomason & Glover, 2008). Similarly, a mix of expiration or inspiration before BH within and between participants potentially added to variability. More controlled/trained breathing may have reduced variability within participants (Thomason & Glover, 2008). However, participants were trained to perform the task before the scan to minimize variations in performance. Accurate end-tidal CO_2 data would have enabled a validity check but were not available.

Second, a BH block of 15 seconds may have been too short to elicit a strong and stable BOLD response in older adults, particularly in the patient group. Prior aging studies employed blocks of 20 seconds (Kannurpatti et al., 2010) and 30 seconds (Riecker et al., 2003), which resulted in less variable brain activation estimates. This is in line with a study comparing 9, 15, and 21 seconds of breath-holding, where 15 seconds blocks were associated with acceptable inter-session reproducibility and inter-trial stability (Magon et al., 2009). While 21 seconds blocks were superior in terms of reduced variability and reproducibility of the response magnitude, participants reported that holding their breath for that long was difficult and led to more chest movement, which may hamper task compliance in older adult groups (Magon et al., 2009). Overall, that study suggested 15 seconds BH durations for calibration studies. Future studies should investigate different BH durations in older adults, particularly patient populations, to devise more efficient and suitable hypercapnic challenges.

Third, uncontrolled pharmacological effects may have influenced the results. Participants in both groups were prescribed medications (e.g., antihypertensives) that may have had an effect on cerebral blood flow, volume, and vessel compliance, and ultimately the hemodynamic response. However, BH hypercapnia scaling is intended to normalize a variety of BOLD signal confounds, including such potential medication effects.

Fourth, causal inferences cannot be drawn since a cross-sectional design was used. As such, there may be factors other than CVD-related alterations in CVR that underlie the whole-brain between-group finding. However, the observed cluster was located in a task-related region, which is consistent with prior research in older adults with cerebral amyloid angiopathy, who demonstrated a reduced BOLD percent signal change in visual cortex in response to a similar paradigm (Dumas et al., 2012; Peca et al., 2013). These patterns of brain activation were related to compromised CVR and white matter damage in the patient group. Future studies may wish to employ a longitudinal design to track disease progression.

Finally, the sample sizes in the present study are small and subsequent studies may profit from increasing the sample size to uncover subtle group differences.

Future Directions

Our results from a simple perception task are very encouraging. Future investigations may compare BH hypercapnia to CO_2 inhalation, a standardized CVR measure, in older adults with CVD. An important aspect of the present study is the simplicity of the BH acquisition and scaling operation, and as such would be ideal as a routine vascular correction method in cognitive fMRI studies in older adult populations.

Providing validation for the use of BH hypercapnia challenges to measure CVR capacity similar to CO_2 inhalation in individuals with CVD would encourage implementation. Other validation approaches should include the collection of end-tidal CO_2 data and examination of relationships with disease or vascular risk factors. Furthermore, the heterogeneous nature of our study samples, including participants with various CVD subgroups, vascular risk factors, and comorbidities, may have added to the variability in the BH data and potentially occluded results. Future studies may benefit from applying this research to more homogenous samples.

Extending the current methods to higher-order cognitive paradigms in order to improve cognitive assessments in fMRI studies of patients with CVD and similar populations is the ultimate goal of this line of research. An ideal candidate would be the n-back paradigm, as it also has well-established activation patterns and cognitive load can be parametrically varied. Applying BH scaling to parametrically varying levels of brain activation (i.e., the different task levels) may provide a deeper understanding of the contributions of underlying metabolic activity versus vascular reactivity. Similarly, acquiring more imaging runs of the cognitive task may enable a test-retest investigation to examine reliability of the scaling operation. Changes in the relationships between brain activation and behavioral performance may provide yet another form of validation. Similarly, extending BH scaling from a simple VS paradigm to other tasks and networks can provide more differentiated information on vascular variability among brain regions and between groups (Buckner et al., 2000; Handwerker et al., 2007; Kannurpatti et al., 2011a; Peca et al., 2013).

Conclusion

The present study appears to be the first to have extended BH hypercapnia scaling to a group of older adults with CVD, and more generally appears to be the first to employ a CVR correction method with the aim to improve the validity of BOLD fMRI in this population. Information on alterations in the cerebrovasculature due to age and disease are not generally included in the analyses of fMRI data in older adult populations, although strong evidence clearly indicates the need. Hypothesis-testing yielded mixed results with brain activation estimates being significantly reduced after scaling, which is a replication of prior scaling studies, while changes in activation extent were not investigated due to spuriously high percent signal changes after scaling. These spurious values also increased, rather than decreased, the variability. Scaling did not have differential effects on CVD patients relative to control participants in ROI analyses. Across the whole brain, evidence for scaling-induced reductions in VS amplitude, extent, and variability were observed, and a cluster of significantly different activation patterns was revealed between groups after scaling. In contrast to prior studies, which have largely restricted their investigations to ROIs, the compelling global observations reported here attest to the relevance of including whole-brain scaling as a complementary analysis. The present findings highlight that conclusions derived from BOLD fMRI studies in older adult populations need to be cautiously interpreted, and provide evidence for the utility and feasibility of incorporating a simple hypercapnia-based correction method in routine fMRI pipelines. As such, BH scaling presents as a convenient way to improve inferences in cognitive studies using BOLD fMRI in older adult populations, especially those with compromised vascular function. More research

is needed to better understand the complex vascular effects on the BOLD signal in older adults with CVD.

REFERENCES

Abbott, D. F., Opdam, H. I., Briellmann, R. S., & Jackson, G. D. (2005). Brief breath holding may confound functional magnetic resonance imaging studies. *Human Brain Mapping, 24*(4), 284-290. doi: Doi 10.1002/Hbm.20086

Alosco, M. L., Gunstad, J., Jerskey, B. A., Clark, U. S., Hassenstab, J. J., Xu, X. M., . . . Sweet, L. H. (2013). Left atrial size is independently associated with cognitive function. *International Journal of Neuroscience, 123*(8), 544-552. doi: Doi 10.3109/00207454.2013.774396

Ances, B. M., Liang, C. L., Leontiev, O., Perthen, J. E., Fleisher, A. S., Lansing, A. E., & Buxton, R. B. (2009). Effects of aging on cerebral blood flow, oxygen metabolism, and blood oxygenation level dependent responses to visual stimulation. *Human Brain Mapping, 30*(4), 1120-1132. doi: 10.1002/hbm.20574

Bandettini, P. A., & Wong, E. C. (1997). A hypercapnia-based normalization method for improved spatial localization of human brain activation with fMRI. *NMR in Biomedicine, 10*(4-5), 197-203.

Belardinelli, R., Georgiou, D., Cianci, G., & Purcaro, A. (1999). Randomized, controlled trial of long-term moderate exercise training in chronic heart failure: effects on functional capacity, quality of life, and clinical outcome. *Circulation, 99*(9), 1173-1182.

Birn, R. M. (2012). The role of physiological noise in resting-state functional connectivity. *NeuroImage, 62*(2), 864-870. doi: 10.1016/j.neuroimage.2012.01.016

Birn, R. M., Murphy, K., Handwerker, D. A., & Bandettini, P. A. (2009). fMRI in the presence of task-correlated breathing variations. *NeuroImage, 47*(3), 1092-1104. doi: 10.1016/j.neuroimage.2009.05.030

Birn, R. M., Smith, M. A., Jones, T. B., & Bandettini, P. A. (2008). The respiration response function: the temporal dynamics of fMRI signal fluctuations related to changes in respiration. *NeuroImage, 40*(2), 644-654. doi: 10.1016/j.neuroimage.2007.11.059

Biswal, B. B., Kannurpatti, S. S., & Rypma, B. (2007). Hemodynamic scaling of fMRI-BOLD signal: validation of low-frequency spectral amplitude as a scalability factor. *Magnetic Resonance Imaging, 25*(10), 1358-1369. doi: DOI 10.1016/j.mri.2007.03.022

Biswal, B. B., Yetkin, F. Z., Haughton, V. M., & Hyde, J. S. (1995). Functional connectivity in the motor cortex of resting human brain using echo-planar MRI. *Magnetic resonance in medicine, 34*(4), 537-541.

Buckner, R. L., Snyder, A. Z., Sanders, A. L., Raichle, M. E., & Morris, J. C. (2000). Functional brain imaging of young, nondemented, and demented older adults. *Journal of Cognitive Neuroscience, 12 Suppl 2*(Supplement 2), 24-34. doi: 10.1162/089892900564046

Chang, C., Thomason, M. E., & Glover, G. H. (2008). Mapping and correction of vascular hemodynamic latency in the BOLD signal. *NeuroImage, 43*(1), 90-102. doi: 10.1016/j.neuroimage.2008.06.030

Chang, T. Y., Liu, H. L., Lee, T. H., Kuan, W. C., Chang, C. H., Wu, H. C., . . . Chang, Y. J. (2009). Change in Cerebral Perfusion after Carotid Angioplasty with Stenting Is Related to Cerebral Vasoreactivity: A Study Using Dynamic Susceptibility-Weighted Contrast-Enhanced MR Imaging and Functional MR Imaging with a Breath-Holding Paradigm. *American Journal of Neuroradiology, 30*(7), 1330-1336. doi: Doi 10.3174/Ajnr.A1589

Changyong, F., Hongyue, W., Naiji, L., Tian, C., Hua, H., & Ying, L. (2014). Log-transformation and its implications for data analysis. *Shanghai Archives of Psychiatry, 26*(2), 105.

Chen, G., Saad, Z. S., Nath, A. R., Beauchamp, M. S., & Cox, R. W. (2012). FMRI group analysis combining effect estimates and their variances. *NeuroImage, 60*(1), 747-765. doi: DOI 10.1016/j.neuroimage.2011.12.060

Cohen, R. A., & Gunstad, J. (Eds.). (2009). *Neuropsychology of Cardiovascular Disease*: Oxford University Press: New York.

Cohen, R. A., Poppas, A., Forman, D. E., Hoth, K. F., Haley, A. P., Gunstad, J., . . . Gerhard-Herman, M. (2009). Vascular and cognitive functions associated with cardiovascular disease in the elderly. *Journal of Clinical and Experimental Neuropsychology, 31*(1), 96-110. doi: 10.1080/13803390802014594

Cohen, R. A., & Sweet, L. H. (2010). *Brain Imaging in Behavioral Medicine and Clinical Neuroscience*: Springer Science & Business Media.

Corfield, D. R., Murphy, K., Josephs, O., Adams, L., & Turner, R. (2001). Does hypercapnia-induced cerebral vasodilation modulate the hemodynamic response to neural activation? *Neuroimage, 13*(6), 1207-1211.

Cox, R. W. (1996). AFNI: software for analysis and visualization of functional magnetic resonance neuroimages. *Computers and Biomedical Research, 29*(3), 162-173.

D'Esposito, M., Deouell, L. Y., & Gazzaley, A. (2003). Alterations in the BOLD fMRI signal with ageing and disease: a challenge for neuroimaging. *Nature Reviews Neuroscience, 4*(11), 863-872. doi: 10.1038/nrn1246

D'Esposito, M., Zarahn, E., Aguirre, G. K., & Rypma, B. (1999). The effect of normal aging on the coupling of neural activity to the bold hemodynamic response. *NeuroImage, 10*(1), 6-14. doi: 10.1006/nimg.1999.0444

Dharmashankar, K., & Widlansky, M. E. (2010). Vascular endothelial function and hypertension: insights and directions. *Current Hypertension Reports, 12*(6), 448-455. doi: 10.1007/s11906-010-0150-2

Di, X., Kannurpatti, S. S., Rypma, B., & Biswal, B. B. (2013). Calibrating BOLD fMRI activations with neurovascular and anatomical constraints. *Cerebral Cortex, 23*(2), 255-263. doi: 10.1093/cercor/bhs001

Donahue, M. J., Stevens, R. D., de Boorder, M., Pekar, J. J., Hendrikse, J., & van Zijl, P. C. (2009). Hemodynamic changes after visual stimulation and breath holding provide evidence for an uncoupling of cerebral blood flow and volume from oxygen metabolism. *Journal of Cerebral Blood Flow & Metabolism, 29*(1), 176-185. doi: 10.1038/jcbfm.2008.109

Dumas, A., Dierksen, G. A., Gurol, M. E., Halpin, A., Martinez-Ramirez, S., Schwab, K., . . . Greenberg, S. M. (2012). Functional magnetic resonance imaging detection of vascular reactivity in cerebral amyloid angiopathy. *Annals of Neurology, 72*(1), 76-81. doi: 10.1002/ana.23566

Faul, F., Erdfelder, E., Lang, A. G., & Buchner, A. (2007). G*Power 3: a flexible statistical power analysis program for the social, behavioral, and biomedical sciences. *Behavior Research Methods, 39*(2), 175-191.

Ferreira, L. K., & Busatto, G. F. (2013). Resting-state functional connectivity in normal brain aging. *Neuroscience & Biobehavioral Reviews, 37*(3), 384-400. doi: 10.1016/j.neubiorev.2013.01.017

Fierstra, J., Sobczyk, O., Battisti-Charbonney, A., Mandell, D. M., Poublanc, J., Crawley, A. P., . . . Fisher, J. A. (2013). Measuring cerebrovascular reactivity: what stimulus to use? *The Journal of Physiology, 591*(23), 5809-5821.

Flück, D., Beaudin, A. E., Steinback, C. D., Kumarpillai, G., Shobha, N., McCreary, C. R., . . . Poulin, M. J. (2014). Effects of aging on the association between cerebrovascular responses to visual stimulation, hypercapnia and arterial stiffness. *Frontiers in Physiology, 5*.

Gati, J. S., Menon, R. S., Ugurbil, K., & Rutt, B. K. (1997). Experimental determination of the BOLD field strength dependence in vessels and tissue. *Magnetic Resonance in Medicine, 38*(2), 296-302.

Gauthier, C. J., Madjar, C., Desjardins-Crepeau, L., Bellec, P., Bherer, L., & Hoge, R. D. (2013). Age dependence of hemodynamic response characteristics in human functional magnetic resonance imaging. *Neurobiology of Aging, 34*(5), 1469-1485. doi: 10.1016/j.neurobiolaging.2012.11.002

Georgiadis, D., Sievert, M., Cencetti, S., Uhlmann, F., Krivokuca, M., Zierz, S., & Werdan, K. (2000). Cerebrovascular reactivity is impaired in patients with cardiac failure. *European Heart Journal, 21*(5), 407-413. doi: DOI 10.1053/euhj.1999.1742

Girouard, H., & Iadecola, C. (2006). Neurovascular coupling in the normal brain and in hypertension, stroke, and Alzheimer disease. *Journal of Applied Physiology, 100*(1), 328-335. doi: 10.1152/japplphysiol.00966.2005

Gonzales, M. M., Tarumi, T., Mumford, J. A., Ellis, R. C., Hungate, J. R., Pyron, M., . . . Haley, A. P. (2014). Greater BOLD response to working memory in endurance-trained adults revealed by breath-hold calibration. *Human Brain Mapping, 35*(7), 2898-2910. doi: 10.1002/hbm.22372

Haley, A. P., Sweet, L. H., Gunstad, J., Forman, D. E., Poppas, A., Paul, R. H., . . . Cohen, R. A. (2007). Verbal working memory and atherosclerosis in patients with cardiovascular disease: an fMRI study. *Journal of Neuroimaging, 17*(3), 227-233. doi: 10.1111/j.1552-6569.2007.00110.x

Hamzei, F., Knab, R., Weiller, C., & Röther, J. (2003). The influence of extra- and intracranial artery disease on the BOLD signal in FMRI. *NeuroImage, 20*(2), 1393-1399. doi: 10.1016/S1053-8119(03)00384-7

Handwerker, D. A., Gazzaley, A., Inglis, B. A., & D'Esposito, M. (2007). Reducing vascular variability of fMRI data across aging populations using a breathholding task. *Human Brain Mapping, 28*(9), 846-859. doi: Doi 10.1002/Hbm.20307

Hedden, T., & Gabrieli, J. D. E. (2004). Insights into the ageing mind: A view from cognitive neuroscience. *Nature Reviews Neuroscience, 5*(2), 87-U12. doi: Doi 10.1038/Nrn1323

Heeger, D. J., & Ress, D. (2002). What does fMRI tell us about neuronal activity? *Nature Reviews Neuroscience, 3*(2), 142-151.

Hesselmann, V., Zaro Weber, O., Wedekind, C., Krings, T., Schulte, O., Kugel, H., . . . Lackner, K. J. (2001). Age related signal decrease in functional magnetic resonance imaging during motor stimulation in humans. *Neuroscience Letters, 308*(3), 141-144.

Huettel, S. A., Singerman, J. D., & McCarthy, G. (2001). The effects of aging upon the hemodynamic response measured by functional MRI. *NeuroImage, 13*(1), 161-175. doi: DOI 10.1006/nimg.2000.0675

Iadecola, C. (2004). Neurovascular regulation in the normal brain and in Alzheimer's disease. *Nature Reviews Neuroscience, 5*(5), 347-360. doi: 10.1038/nrn1387

Irani, F., Sweet, L. H., Haley, A. P., Gunstad, J. J., Jerskey, B. A., Mulligan, R. C., . . . Cohen, R. A. (2009). A fMRI Study of Verbal Working Memory, Cardiac Output, and Ejection Fraction in Elderly Patients with Cardiovascular Disease. *Brain Imaging and Behavior, 3*(4), 350-357.

Jefferson, A. L., Hohman, T. J., Liu, D., Haj-Hassan, S., Gifford, K. A., Benson, E. M., . . . Sumner, E. C. (2014). Adverse Vascular Risk is Related to Cognitive Decline in Older Adults. *Journal of Alzheimer's Disease*.

Jefferson, A. L., Holland, C. M., Tate, D. F., Csapo, I., Poppas, A., Cohen, R. A., & Guttmann, C. R. (2011). Atlas-derived perfusion correlates of white matter hyperintensities in patients with reduced cardiac output. *Neurobiology of Aging, 32*(1), 133-139. doi: 10.1016/j.neurobiolaging.2009.01.011

Jefferson, A. L., Tate, D. F., Poppas, A., Brickman, A. M., Paul, R. H., Gunstad, J., & Cohen, R. A. (2007). Lower cardiac output is associated with greater white matter hyperintensities in older adults with cardiovascular disease. *Journal of the American Geriatrics Society, 55*(7), 1044-1048. doi: DOI 10.1111/j.1532-5415.2007.01226.x

Kannurpatti, S. S., & Biswal, B. B. (2008). Detection and scaling of task-induced fMRI-BOLD response using resting state fluctuations. *NeuroImage, 40*(4), 1567-1574. doi: DOI 10.1016/j.neuroimage.2007.09.040

Kannurpatti, S. S., Motes, M. A., Rypma, B., & Biswal, B. B. (2010). Neural and vascular variability and the fMRI-BOLD response in normal aging. *Magnetic Resonance Imaging, 28*(4), 466-476. doi: 10.1016/j.mri.2009.12.007

Kannurpatti, S. S., Motes, M. A., Rypma, B., & Biswal, B. B. (2011a). Increasing measurement accuracy of age-related BOLD signal change: minimizing vascular contributions by resting-state-fluctuation-of-amplitude scaling. *Human Brain Mapping, 32*(7), 1125-1140. doi: 10.1002/hbm.21097

Kannurpatti, S. S., Motes, M. A., Rypma, B., & Biswal, B. B. (2011b). Non-neural BOLD variability in block and event-related paradigms. *Magnetic Resonance Imaging, 29*(1), 140-146. doi: 10.1016/j.mri.2010.07.006

Kastrup, A., Dichgans, J., Niemeier, M., & Schabet, M. (1998). Changes of cerebrovascular CO2 reactivity during normal aging. *Stroke, 29*(7), 1311-1314.

Kastrup, A., Kruger, G., Glover, G. H., & Moseley, M. E. (1999). Assessment of cerebral oxidative metabolism with breath holding and fMRI. *Magnetic Resonance in Medicine, 42*(3), 608-611.

Kastrup, A., Kruger, G., Glover, G. H., Neumann-Haefelin, T., & Moseley, M. E. (1999). Regional variability of cerebral blood oxygenation response to hypercapnia. *NeuroImage, 10*(6), 675-681. doi: 10.1006/nimg.1999.0505

Kastrup, A., Kruger, G., Neumann-Haefelin, T., & Moseley, M. E. (2001). Assessment of cerebrovascular reactivity with functional magnetic resonance imaging: comparison of CO(2) and breath holding. *Magnetic Resonance Imaging, 19*(1), 13-20.

Knopman, D., Boland, L. L., Mosley, T., Howard, G., Liao, D., Szklo, M., . . . Folsom, A. R. (2001). Cardiovascular risk factors and cognitive decline in middle-aged adults. *Neurology, 56*(1), 42-48.

Krainik, A., Hund-Georgiadis, M., Zysset, S., & von Cramon, D. Y. (2005). Regional impairment of cerebrovascular reactivity and BOLD signal in adults after stroke. *Stroke, 36*(6), 1146-1152. doi: 10.1161/01.STR.0000166178.40973.a7

Kwong, K. K., Belliveau, J. W., Chesler, D. A., Goldberg, I. E., Weisskoff, R. M., Poncelet, B. P., . . . et al. (1992). Dynamic magnetic resonance imaging of human brain activity during primary sensory stimulation. *Proceedings of the National Academy of Sciences, 89*(12), 5675-5679.

Lakens, D. (2013). Calculating and reporting effect sizes to facilitate cumulative science: a practical primer for t-tests and ANOVAs. *Frontiers in Psychology, 4*, 863. doi: 10.3389/fpsyg.2013.00863

Last, D., Alsop, D. C., Abduljalil, A. M., Marquis, R. P., de Bazelaire, C., Hu, K., . . . Novak, V. (2007). Global and regional effects of type 2 diabetes on brain tissue volumes and cerebral vasoreactivity. *Diabetes Care, 30*(5), 1193-1199. doi: 10.2337/dc06-2052

Leoni, R. F., Mazzeto-Betti, K. C., Andrade, K. C., & de Araujo, D. B. (2008). Quantitative evaluation of hemodynamic response after hypercapnia among different brain territories by fMRI. *NeuroImage, 41*(4), 1192-1198. doi: DOI 10.1016/j.neuroimage.2008.03.035

Leoni, R. F., Mazzetto-Betti, K. C., Silva, A. C., dos Santos, A. C., de Araujo, D. B., Leite, J. P., & Pontes-Neto, O. M. (2012). Assessing cerebrovascular reactivity in carotid steno-occlusive disease using MRI BOLD and ASL techniques. *Radiology Research and Practice, 2012*.

Leritz, E. C., Salat, D. H., Williams, V. J., Schnyer, D. M., Rudolph, J. L., Lipsitz, L., . . . Milberg, W. P. (2011). Thickness of the human cerebral cortex is associated with metrics of

cerebrovascular health in a normative sample of community dwelling older adults. *NeuroImage, 54*(4), 2659-2671. doi: DOI 10.1016/j.neuroimage.2010.10.050

Li, T. Q., Kastrup, A., Takahashi, A. M., & Moseley, M. E. (1999). Functional MRI of human brain during breath holding by BOLD and FAIR techniques. *NeuroImage, 9*(2), 243-249. doi: 10.1006/nimg.1998.0399

Liu, H. L., Huang, Ju, Wu, C. T., & Hsu, Y. Y. (2002). Detectability of blood oxygenation level-dependent signal changes during short breath hold duration. *Magnetic Resonance Imaging, 20*(9), 643-648.

Lythgoe, D. J., Williams, S. C. R., Cullinane, M., & Markus, H. S. (1999). Mapping of cerebrovascular reactivity using bold magnetic resonance imaging. *Magnetic Resonance Imaging, 17*(4), 495-502. doi: Doi 10.1016/S0730-725x(98)00211-2

Magon, S., Basso, G., Farace, P., Ricciardi, G. K., Beltramello, A., & Sbarbati, A. (2009). Reproducibility of BOLD signal change induced by breath holding. *NeuroImage, 45*(3), 702-712. doi: 10.1016/j.neuroimage.2008.12.059

Mark, C. I., Mazerolle, E. L., & Chen, J. J. (2015). Metabolic and vascular origins of the BOLD effect: Implications for imaging pathology and resting-state brain function. *Journal of Magnetic Resonance Imaging*. doi: 10.1002/jmri.24786

Markus, H., & Cullinane, M. (2001). Severely impaired cerebrovascular reactivity predicts stroke and TIA risk in patients with carotid artery stenosis and occlusion. *Brain, 124*(Pt 3), 457-467.

Markus, H.S., & Harrison, M.J.G. (1992). Estimation of Cerebrovascular Reactivity Using Transcranial Doppler, Including the Use of Breath-Holding as the Vasodilatory Stimulus. *Stroke, 23*(5), 668-673.

Menon, R. S. (2001). Imaging function in the working brain with fMRI. *Current Opinion in Neurobiology, 11*(5), 630-636.

Meusel, L. A., Kansal, N., Tchistiakova, E., Yuen, W., MacIntosh, B. J., Greenwood, C. E., & Anderson, N. D. (2014). A systematic review of type 2 diabetes mellitus and hypertension in imaging studies of cognitive aging: time to establish new norms. *Frontiers in Aging Neuroscience, 6*, 148. doi: 10.3389/fnagi.2014.00148

Miller, L. A., Spitznagel, M. B., Alosco, M. L., Cohen, R. A., Raz, N., Sweet, L. H., . . . Gunstad, J. (2012). Cognitive profiles in heart failure: a cluster analytic approach. *Journal of Clinical and Experimental Neuropsychology, 34*(5), 509-520. doi: 10.1080/13803395.2012.663344

Mozaffarian, D., Benjamin, E. J., Go, A. S., Arnett, D. K., Blaha, M. J., Cushman, M., . . . Howard, V. J. (2015). Heart Disease and Stroke Statistics—2015 Update A Report From the American Heart Association. *Circulation, 131*(4), e29-e322.

Murphy, K., Harris, A. D., & Wise, R. G. (2011). Robustly measuring vascular reactivity differences with breath-hold: normalising stimulus-evoked and resting state BOLD fMRI data. *NeuroImage, 54*(1), 369-379. doi: 10.1016/j.neuroimage.2010.07.059

Murphy, S. L., Xu, J., & Kochanek, K. D. (2013). National vital statistics reports. *National Vital Statistics Reports, 61*(4).

Peca, S., McCreary, C. R., Donaldson, E., Kumarpillai, G., Shobha, N., Sanchez, K., . . . Smith, E. E. (2013). Neurovascular decoupling is associated with severity of cerebral amyloid angiopathy. *Neurology, 81*(19), 1659-1665.

Pineiro, R, Pendlebury, S, Johansen-Berg, H, & Matthews, PM. (2002). Altered hemodynamic responses in patients after subcortical stroke measured by functional MRI. *Stroke, 33*(1), 103-109.

Portegies, M. L., de Bruijn, R. F., Hofman, A., Koudstaal, P. J., & Ikram, M. A. (2014). Cerebral vasomotor reactivity and risk of mortality: the Rotterdam Study. *Stroke, 45*(1), 42-47. doi: 10.1161/STROKEAHA.113.002348

Raichle, M. E., MacLeod, A. M., Snyder, A. Z., Powers, W. J., Gusnard, D. A., & Shulman, G. L. (2001). A default mode of brain function. *Proceedings of the National Academy of Sciences, 98*(2), 676-682. doi: 10.1073/pnas.98.2.676

Riecker, A., Grodd, W., Klose, U., Schulz, J. B., Gröschel, K., Erb, M., . . . Kastrup, A. (2003). Relation between regional functional MRI activation and vascular reactivity to carbon dioxide during normal aging. *Journal of Cerebral Blood Flow and Metabolism, 23*(5), 565-573. doi: Doi 10.1097/01.Wcb.0000056063.25434.04

Rossini, P. M., Altamura, C., Ferretti, A., Vernieri, F., Zappasodi, F., Caulo, M., . . . Tecchio, F. (2004). Does cerebrovascular disease affect the coupling between neuronal activity and local haemodynamics? *Brain, 127*(1), 99-110.

Röther, J., Knab, R., Hamzei, F., Fiehler, J., Reichenbach, J. R., Büchel, C., & Weiller, C. (2002). Negative dip in BOLD fMRI is caused by blood flow—oxygen consumption uncoupling in humans. *NeuroImage, 15*(1), 98-102.

Samanez-Larkin, G. R., & D'Esposito, M. (2008). Group comparisons: imaging the aging brain. *Social Cognitive and Affective Neuroscience, 3*(3), 290-297. doi: 10.1093/scan/nsn029

Silvestrini, M., Pasqualetti, P., Baruffaldi, R., Bartolini, M., Handouk, Y., Matteis, M., . . . Vernieri, F. (2006). Cerebrovascular reactivity and cognitive decline in patients with Alzheimer disease. *Stroke, 37*(4), 1010-1015. doi: 10.1161/01.STR.0000206439.62025.97

Silvestrini, M., Vernieri, F., Pasqualetti, P., Matteis, M., Passarelli, F., Troisi, E., & Caltagirone, C. (2000). Impaired cerebral vasoreactivity and risk of stroke in patients with asymptomatic carotid artery stenosis. *Journal of the American Medical Association, 283*(16), 2122-2127.

Silvestrini, M., Vernieri, F., Troisi, E., Passarelli, F., Matteis, M., Pasqualetti, P., . . . Caltagirone, C. (1999). Cerebrovascular reactivity in carotid artery occlusion: possible implications for

surgical management of selected groups of patients. *Acta Neurologica Scandinavica, 99*(3), 187-191.

Stillman, A. E., Hu, X., & Jerosch-Herold, M. (1995). Functional Mri of Brain during Breath-Holding at 4-T. *Magnetic Resonance Imaging, 13*(6), 893-897. doi: Doi 10.1016/0730-725x(95)00037-H

Tancredi, F. B., & Hoge, R. D. (2013). Comparison of cerebral vascular reactivity measures obtained using breath-holding and CO2 inhalation. *Journal of Cerebral Blood Flow and Metabolism, 33*(7), 1066-1074. doi: DOI 10.1038/jcbfm.2013.48

Tchistiakova, E., Anderson, N. D., Greenwood, C. E., & MacIntosh, B. J. (2014). Combined effects of type 2 diabetes and hypertension associated with cortical thinning and impaired cerebrovascular reactivity relative to hypertension alone in older adults. *NeuroImage: Clinical, 5*, 36-41. doi: 10.1016/j.nicl.2014.05.020

Team, R Core. (2014). R: A language and environment for statistical computing. R Foundation for Statistical Computing, Vienna, Austria, 2012: ISBN 3-900051-07-0.

Thomason, M. E., Burrows, B. E., Gabrieli, J. D., & Glover, G. H. (2005). Breath holding reveals differences in fMRI BOLD signal in children and adults. *NeuroImage, 25*(3), 824-837. doi: 10.1016/j.neuroimage.2004.12.026

Thomason, M. E., Foland, L. C., & Glover, G. H. (2007). Calibration of BOLD fMRI using breath holding reduces group variance during a cognitive task. *Human Brain Mapping, 28*(1), 59-68. doi: Doi 10.1002/Hbm.20241

Thomason, M. E., & Glover, G. H. (2008). Controlled inspiration depth reduces variance in breath-holding-induced BOLD signal. *NeuroImage, 39*(1), 206-214. doi: 10.1016/j.neuroimage.2007.08.014

Van der Zande, F. H. R., Hofman, P. A. M., & Backes, W. H. (2005). Mapping hypercapnia-induced cerebrovascular reactivity using BOLD MRI. *Neuroradiology, 47*(2), 114-120.

Vernieri, F., Pasqualetti, P., Matteis, M., Passarelli, F., Troisi, E., Rossini, P. M., . . . Silvestrini, M. (2001). Effect of collateral blood flow and cerebral vasomotor reactivity on the outcome of carotid artery occlusion. *Stroke, 32*(7), 1552-1558.

Wilson, S. M. (2014). The impact of vascular factors on language localization in the superior temporal sulcus. *Human Brain Mapping, 35*(8), 4049-4063. doi: 10.1002/hbm.22457

Yuan, R., Di, X., Kim, E. H., Barik, S., Rypma, B., & Biswal, B. B. (2013). Regional homogeneity of resting-state fMRI contributes to both neurovascular and task activation variations. *Magnetic Resonance Imaging, 31*(9), 1492-1500. doi: DOI 10.1016/j.mri.2013.07.005

Zeki, S., Watson, J. D., Lueck, C. J., Friston, K. J., Kennard, C., & Frackowiak, R. S. (1991). A direct demonstration of functional specialization in human visual cortex. *Journal of Neuroscience, 11*(3), 641-649.

Table 1

Sample Characteristics

Patient Group									
Participant	Age (years)	Risk Factor (Type)	Medication (Type)	ROI Volume^{o}	BH^	Unscaled VS^	Scaled VS^	Pre-Scaling Correlation*	Post-Scaling Correlation*
1	77	CAD, D, H, HA	AC, BB, OA, TD	1567	0.40	0.81	0.65	0.59	-0.13
2	60	C, HA	AC	2531	1.01	0.91	0.95	0.72	-0.41
3	59	C, CAD, H	AC, AI, BB, TD	2400	0.91	1.02	0.98	0.23	-0.38
4	81	CAD, HA		943	1.75	1.70	1.60	0.75	-0.61
5	86	C, CAD, H	AC, AI, TD	1114	0.11	1.36	0.46	0.29	0.42
6	83	C, H, HA		1172	0.52	1.21	1.17	0.52	-0.38
7	63	C, H, HA		725	0.89	1.09	1.01	0.63	-0.57
8	60	C, CAD	AC, AI	773	0.43	1.09	0.93	0.57	-0.22
9	64	C, CAD, H	AC, BB	1147	0.52	1.23	1.08	0.33	-0.43
10	71	C, D, H	AC, AI, BB	443	0.11	1.25	0.33	-0.22	0.39
11	73	C, CAD, D, H, HA	AC, BB, CC	1035	1.20	1.44	1.36	0.64	-0.52
12	74	C, H, HA	AC, AI	2037	0.93	1.11	0.99	0.63	-0.56
13	60	C, CAD	AC, BB	1429	1.14	1.16	1.05	0.48	-0.51
14	71			1541	0.42	0.94	0.65	0.15	0.12
M±SD	*70 ± 9*			*1347 ± 620*	*0.74 ± 0.46*	*1.17 ± 0.23*	*0.94 ± 0.34*	*0.45 ± 0.20*	*-0.27 ± 0.35*
CV				*0.46*	*0.62*	*0.20*	*0.36*	*0.44*	1.30

Matched Control Group									
Participant	Age (years)	Diagnosis/Risk Factor (Type)	Medication (Type)	ROI Volume^{o}	BH^	Unscaled VS^	Scaled VS^	Pre-Scaling Correlation*	Post-Scaling Correlation*
1	73	D	AC, BB, CC	1219	1.16	0.80	0.68	0.49	-0.18
2	64	H	AI	2744	0.41	0.96	0.71	0.49	-0.14
3	74	C, H	AI	115	1.63	0.92	0.91	0.72	-0.62
4	73	H	OA	2503	0.22	0.93	0.58	0.23	0.11
5	59	C		1885	0.65	1.02	1.02	0.47	-0.41
6	57	C, H	AI	1703	0.94	1.30	1.16	0.62	-0.40
7	75		AI	885	0.47	1.38	1.25	0.24	-0.32
8	74			813	0.65	1.19	1.15	0.52	-0.34
9	76	C	BB	2851	0.83	0.78	0.74	0.65	-0.36
10	58	C, H	TD	2354	0.66	1.16	0.90	0.09	-0.19
11	58			1955	1.64	0.92	0.86	0.70	-0.41
12	67			1176	0.81	1.48	1.30	0.39	-0.46
13	58			1238	0.71	0.96	0.85	0.76	-0.57
14	66		AC, AI, CC	723	0.65	0.97	0.98	0.56	-0.42
M±SD	*67±7*			*1583±834*	*0.82±0.41*	*1.06±0.21*	*0.94±0.22*	*0.50±0.20*	*-0.34±0.19*
CV				*0.53*	*0.50*	*0.20*	*0.23*	*0.40*	-0.56

Note: BH=breath-hold, VS=visual stimulation, M=mean, SD=standard deviation, CV=coefficient of variation (SD/mean). ºNumber of grey matter voxels of significant positive association with VS at $p<.01$. ^Median percent signal change. *all at $p<.001$. Diagnoses and risk factors (%patients/%matched controls): C=cholesterolemia (79/36%), CAD=coronary artery disease (52/0%), D=diabetes (21/7%), H=hypertension (64/36%), HA=heart attack (50%/0%). AC=Anticoagulant/antiplatelet, AI= ACE inhibitor, BB=Beta-blocker, CC=Calcium-channel blocker, OA=Other Antihypertensive drugs, TD=Thiazide Diuretic. Pre-Scaling Correlation=Pearson's *r* of BH and unscaled VS percent signal change, Post-Scaling Correlation=Spearman's *rho* of BH and scaled VS percent signal change

Table 2

Descriptive Statistics in Functional ROIs

Patient Group												
	Unscaled Visual Stimulation Percent Signal Change						Scaled Visual Stimulation Percent Signal Change					
Participant	Smallest	Largest	Median	MAD	Mean	SD	Smallest	Largest	Median	MAD	Mean	SD
1	0.20	4.04	0.81	0.40	0.96	0.54	-403.90	144.64	0.65	0.51	0.01	15.88
2	0.19	12.78	0.91	0.62	1.28	1.07	-48.24	40.65	0.95	0.51	1.23	2.93
3	0.20	7.68	1.02	0.69	1.23	0.84	-1816.81	1278.77	0.98	0.74	1.62	55.64
4	0.36	7.51	1.70	0.86	2.00	1.13	-114.80	52.32	1.60	0.82	1.66	5.18
5	0.23	11.58	1.36	0.82	1.69	1.32	-252.32	70.22	0.46	1.16	0.13	9.69
6	0.31	6.31	1.21	0.64	1.43	0.89	-213.41	240.41	1.17	0.76	1.50	12.23
7	0.23	4.31	1.09	0.63	1.22	0.68	-66.83	69.12	1.01	0.62	1.28	3.86
8	0.17	6.12	1.09	0.72	1.28	0.83	-354.77	15934.60	0.93	0.76	20.94	573.48
9	0.21	5.83	1.23	0.75	1.39	0.82	-56.67	3285.97	1.08	0.81	4.36	97.14
10	0.31	4.32	1.25	0.72	1.45	0.75	-547.03	81.95	0.33	1.14	-0.62	26.54
11	0.35	7.46	1.44	0.83	1.71	1.07	-2877.37	102.34	1.36	0.82	-0.91	89.73
12	0.25	8.62	1.11	0.67	1.33	0.88	-159.01	131.85	0.99	0.65	1.29	6.68
13	0.19	5.89	1.16	0.69	1.32	0.79	-51.04	460.29	1.05	0.69	1.54	12.28
14	0.19	5.27	0.94	0.58	1.14	0.74	-1129.00	685.99	0.65	0.55	0.09	35.88

Matched Control Group												
	Unscaled Visual Stimulation Percent Signal Change						Scaled Visual Stimulation Percent Signal Change					
Participant	Smallest	Largest	Median	MAD	Mean	SD	Smallest	Largest	Median	MAD	Mean	SD
1	0.21	10.02	0.80	0.54	1.04	0.80	-423.48	68.34	0.68	0.40	0.54	12.94
2	0.25	7.40	0.96	0.61	1.19	0.81	-122.49	1295.65	0.71	0.56	1.69	27.89
3	0.39	2.23	0.92	0.33	0.99	0.37	0.42	1.64	0.91	0.28	0.95	0.30
4	0.19	10.54	0.93	0.59	1.29	1.07	-545.29	1474.26	0.58	0.82	1.11	33.76
5	0.18	6.99	1.02	0.67	1.21	0.79	-35.31	3046.51	1.02	0.71	2.98	70.41
6	0.23	7.22	1.30	0.89	1.62	1.13	-142.04	114.71	1.16	0.71	1.52	5.61
7	0.25	6.15	1.38	0.79	1.59	0.97	-119.65	780.79	1.25	0.88	3.05	30.55
8	0.21	6.85	1.19	0.72	1.42	0.99	-27.07	93.59	1.15	0.68	1.75	5.50
9	0.20	6.72	0.78	0.47	1.08	0.85	-40.01	20.62	0.74	0.40	0.96	1.35
10	0.17	9.06	1.16	0.80	1.45	1.02	-303.36	94.23	0.90	0.75	1.03	10.10
11	0.26	5.20	0.92	0.48	1.12	0.68	-97.30	31.89	0.95	0.42	1.08	2.90
12	0.20	5.83	1.48	1.01	1.66	0.99	-63.54	67.49	1.30	0.88	1.75	3.88
13	0.23	8.35	0.96	0.59	1.32	1.07	-47.14	46.21	0.95	0.52	1.21	2.30
14	0.26	5.63	0.97	0.51	1.17	0.75	-1116.43	20.60	0.98	0.55	-0.42	41.66

Note: Smallest=smallest percent signal change; largest=largest percent signal change; MAD=median absolute deviation; SD=standard deviation

Table 3

Regions of Significant Scaling Effects by Group

Cluster	Region	Coordinates	Number of Voxels
Patient Group			
1	Bilateral lingual gyrus, extending into BA 18, cuneus, and middle occipital gyrus merged with bilateral cingulate gyrus, extending into posterior cingulate and precuneus, BA 7/BA 31	-4 +77 +4	2617
2	Right middle/superior temporal gyrus, extending into precuneus and inferior/superior parietal lobule	-45 +62 +32	265
3	Right superior frontal gyrus/BA 10, extending into middle frontal gyrus	-29 -47 +23	179
4	Right middle temporal gyrus/BA 21/BA 22	-56 +11 -3	165
Matched Control Group			
1	Bilateral Lingual Gyrus/BA 18, extending into Cuneus and BA 17	-2 +82 0	882
2	Cingulate Gyrus extending into Precuneus and BAs 21/7	-2 +56 +29	519
Larger Control Cohort			
1	Bilateral lingual gyrus, extending into BA 18, cuneus, and middle occipital gyrus	-3 +82 -1	1278
2	Bilateral cingulate gyrus, extending into posterior cingulate and precuneus, BA 7/BA 31	-2 +57 +29	1163
3	Left precuneus, extending into inferior and superior parietal lobule, BA 7, BA 39	+36 +69 +41	177
4	Bilateral cingulate, extending into medial frontal gyrus	-1 +3 +48	136
5	Right superior frontal gyrus/BA 10, extending into middle frontal gyrus	-29 -53 +16	133

Note: Clusters obtained from Wilcoxon signed-rank tests in each group. Coordinates XYZ are center of mass in Talairach space. BA=Brodmann Area. Figure 5 provides the corresponding statistical group maps and Figure 6 the median visual stimulation BOLD percent signal changes in these clusters before and after scaling.

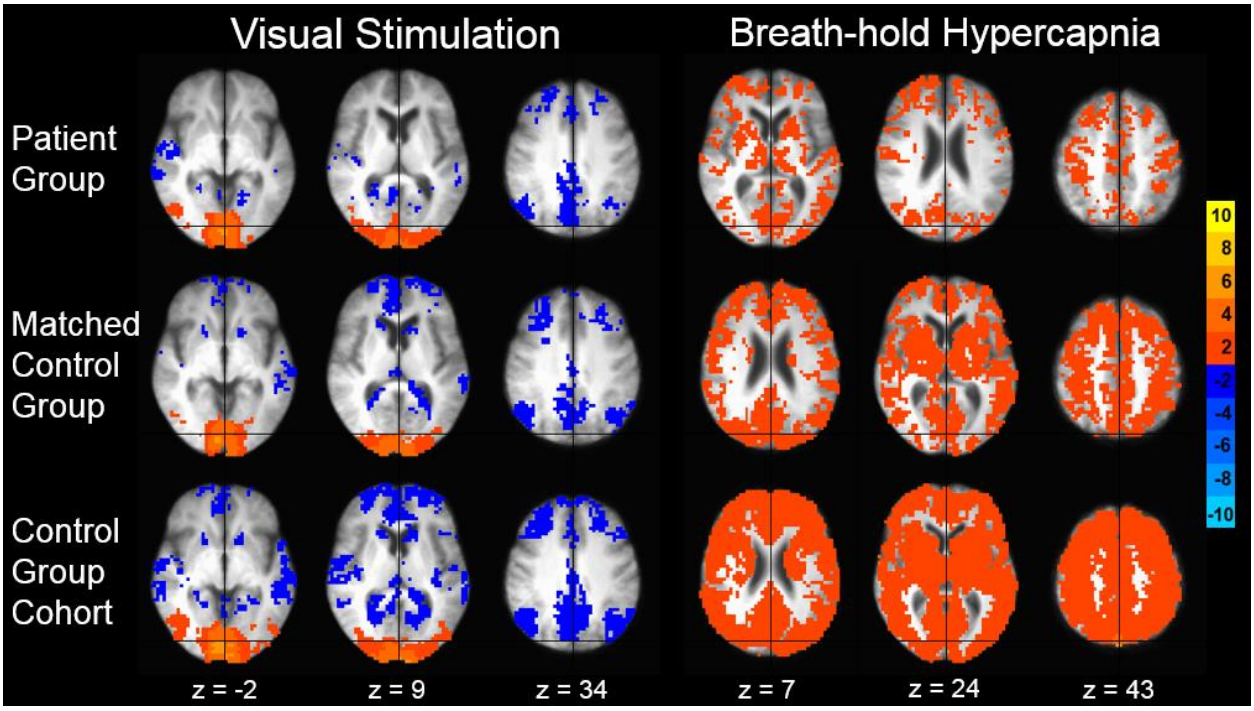

Figure 1
Brain Activation to Visual Stimulation and Breath-hold Hypercapnia

Within-group whole-brain activation maps from mixed-effects models of the visual stimulation vs fixation and the breath-holding vs self-paced breathing contrasts. Shown are β estimates voxel-wise thresholded by *t*-values at $p<.01$ for the visual maps and at a more stringent $p<.001$ for the robust breath-hold maps (all two-tailed and cluster family-wise error corrected at $\alpha<.01$, scale indicates *t*-values). Images are in radiological orientation (left=right) and displayed on axial slices of the respective group-averaged T1-weighted image in Talairach space. Crosshairs are included for comparison with other figures.

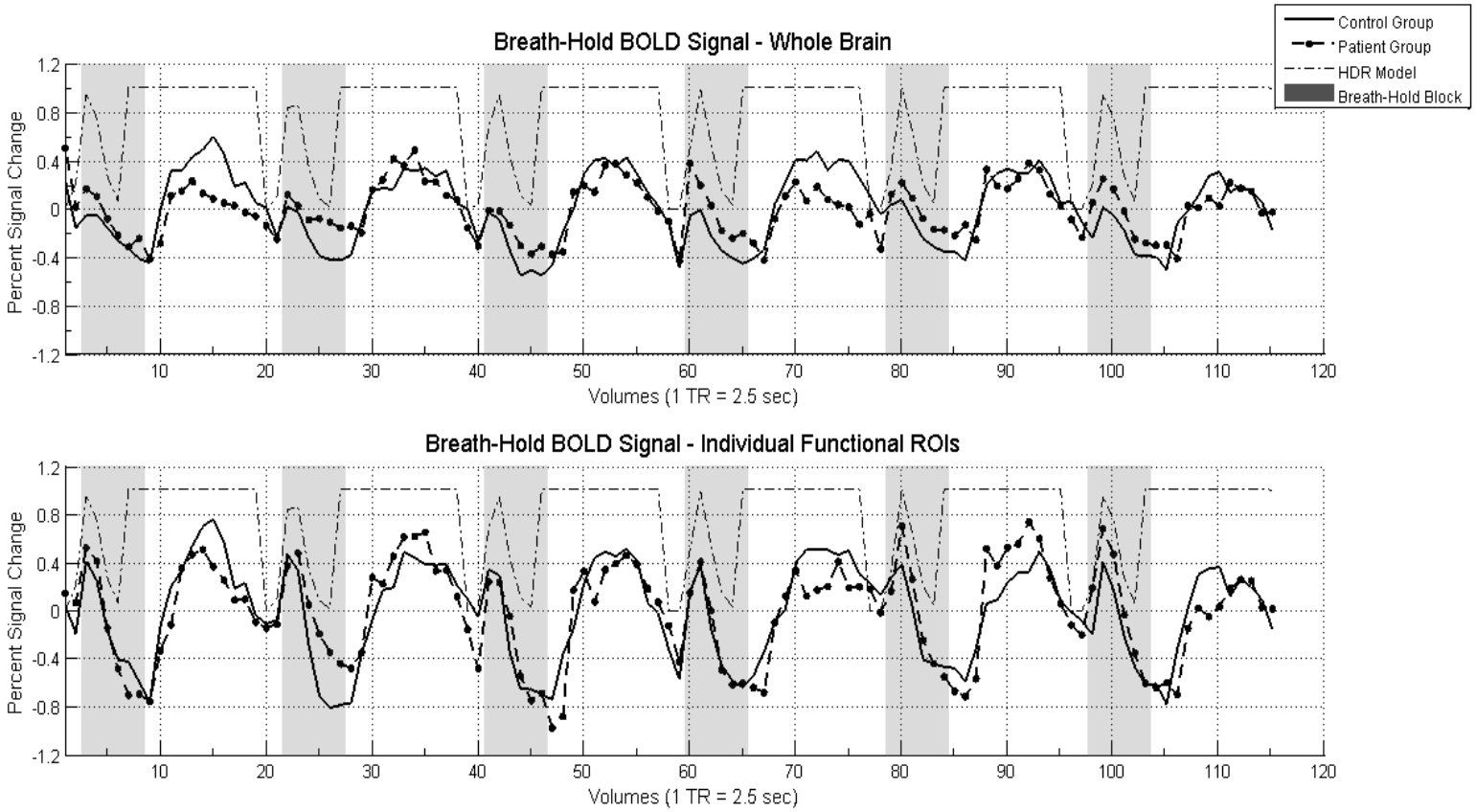

Figure 2
Breath-hold Hypercapnia BOLD Signal across the Whole Brain and in ROIs

Average breath-hold time series were extracted from the whole brain (top) and in the functional grey matter region of interest (ROI) (bottom) of each participant and averaged within the patient and the matched control groups (time-series are slice-time corrected, volume-registered, spatially smoothed with 4 mm full-width at half-maximum Gaussian filter, scaled, and detrended). HDR=hemodynamic response model.

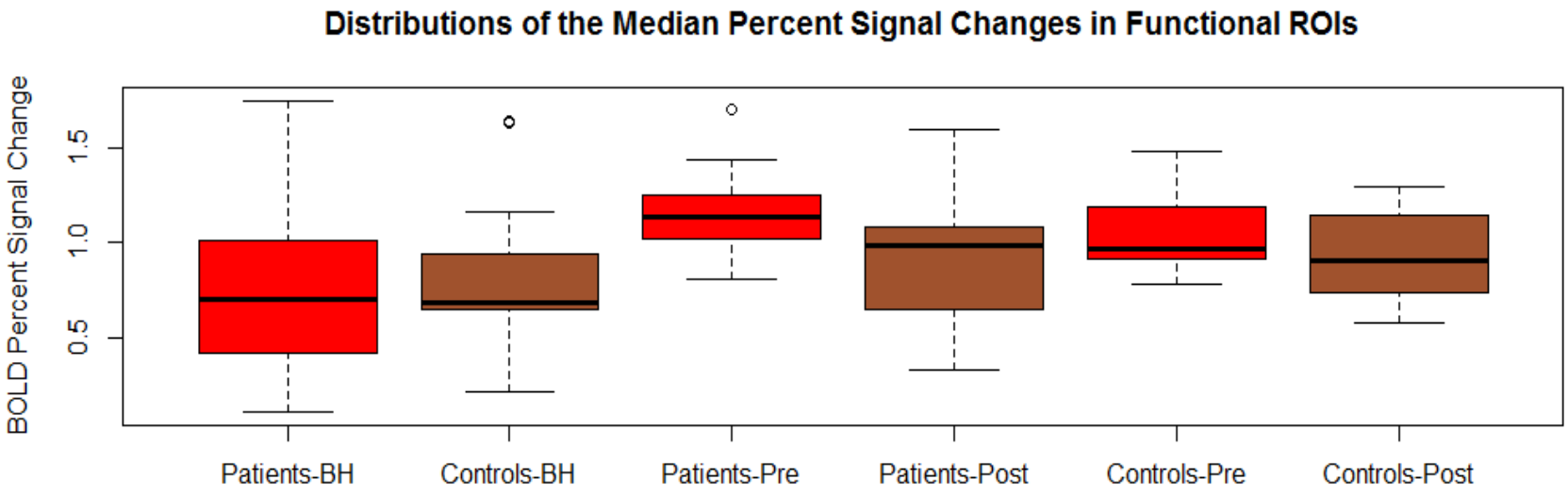

Figure 3
Percent Signal Changes in Functional ROIs

Median percent signal changes in functional grey matter regions of interest (ROI) across groups before and after scaling. BH=breath-hold; Pre=unscaled visual stimulation percent signal change; Post=scaled visual stimulation percent signal change

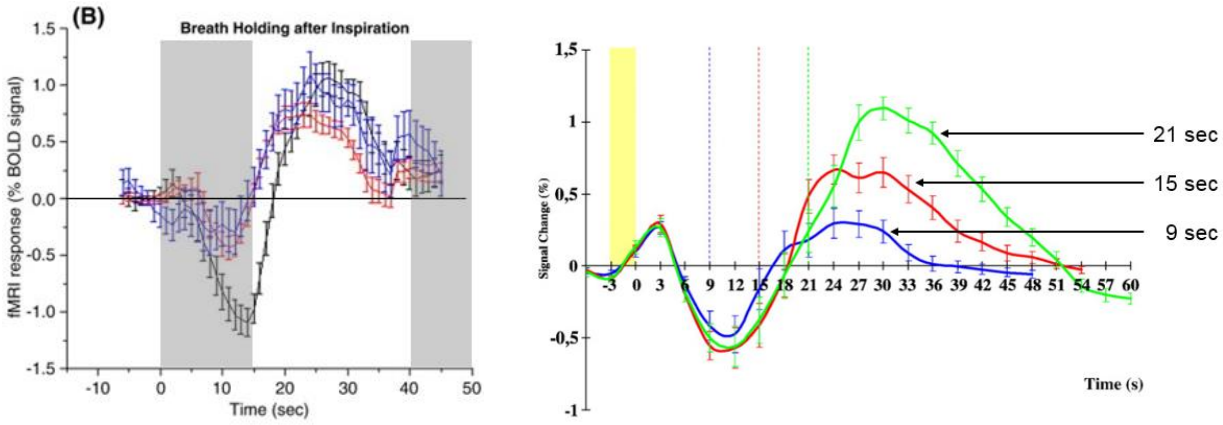

Figure 4
Examples of the Breath-hold BOLD Signal Shape

Shown are two figures from the literature depicting breath-hold (BH) time courses similar to the ones observed in the current study. Below are original figure captions reproduced:

Panel on the left: “Averaged BOLD signal time course with breath holding of 15 s after (…) (B) inspiration on areas supplied by the middle cerebral artery (red), anterior cerebral artery (blue) and posterior cerebral artery (black).” (Leoni et al., 2008) *Note:* Changes made to the original image for inclusion in the above figure include vertical grey bars to indicate the BH block, a line at zero, and spelling out of acronyms for anterior, middle, and posterior arteries in the caption.

Panel on the right: “Average signal change during three BH durations (…) across subjects. The yellow bar indicates the inspiration phase. The BH phase started at time zero; the dotted lines indicated the end of the BH period. (…)” (Magon et al., 2009)

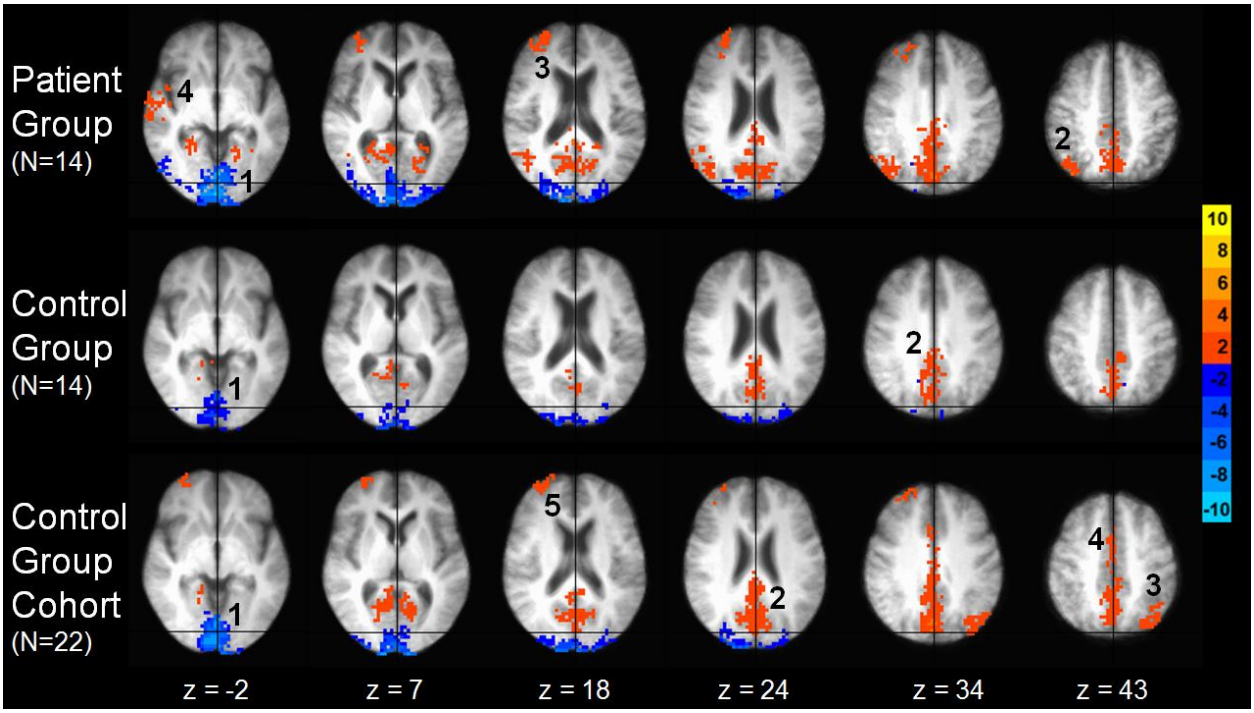

Figure 5
Clusters of Significant Scaling Effects within Groups

Whole-brain Wilcoxon signed-rank tests contrasting the β coefficients for visual stimulation before vs after scaling at a voxel-wise $p<.05$ (two-tailed, cluster family-wise error corrected at $\alpha<.05$, scale indicates the normalized Wilcoxon signed-rank statistics Z). Numbers indicate brain regions detailed in Table 3. Warmer colors express attenuation of brain deactivation and cooler colors express reduction in brain activation after scaling (for details see Figure 6). Statistical images are in radiological orientation (left=right) and displayed on axial slices of the respective group-averaged T1-weighted image in Talairach space. Crosshairs are included for comparison with other figures.

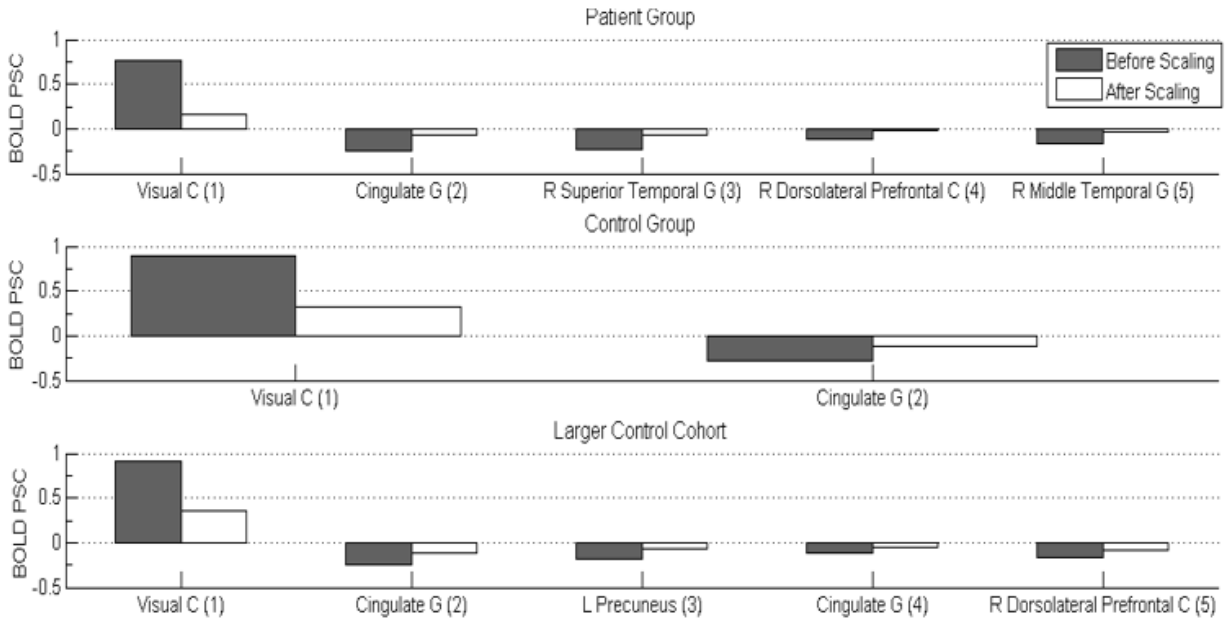

Figure 6

Medians in Clusters of Significant Scaling Effects

Median visual stimulation BOLD percent signal change before and after scaling in clusters obtained with Wilcoxon signed-rank tests in each group. The numbers after each region label indicate the cluster numbers in Table 3 and Figure 5. Note: in the patient group, visual cortex (1) and cingulate gyrus (2) originally comprised one large cluster, containing both positive and negative Wilcoxon signed-rank estimates (Figure 5). This cluster was separated into a negative visual cortex and a positive cingulate gyrus cluster to better reflect median percent signal changes. PSC=Percent Signal Change, C=Cortex, G=Gyrus, R=Right, L=Left.

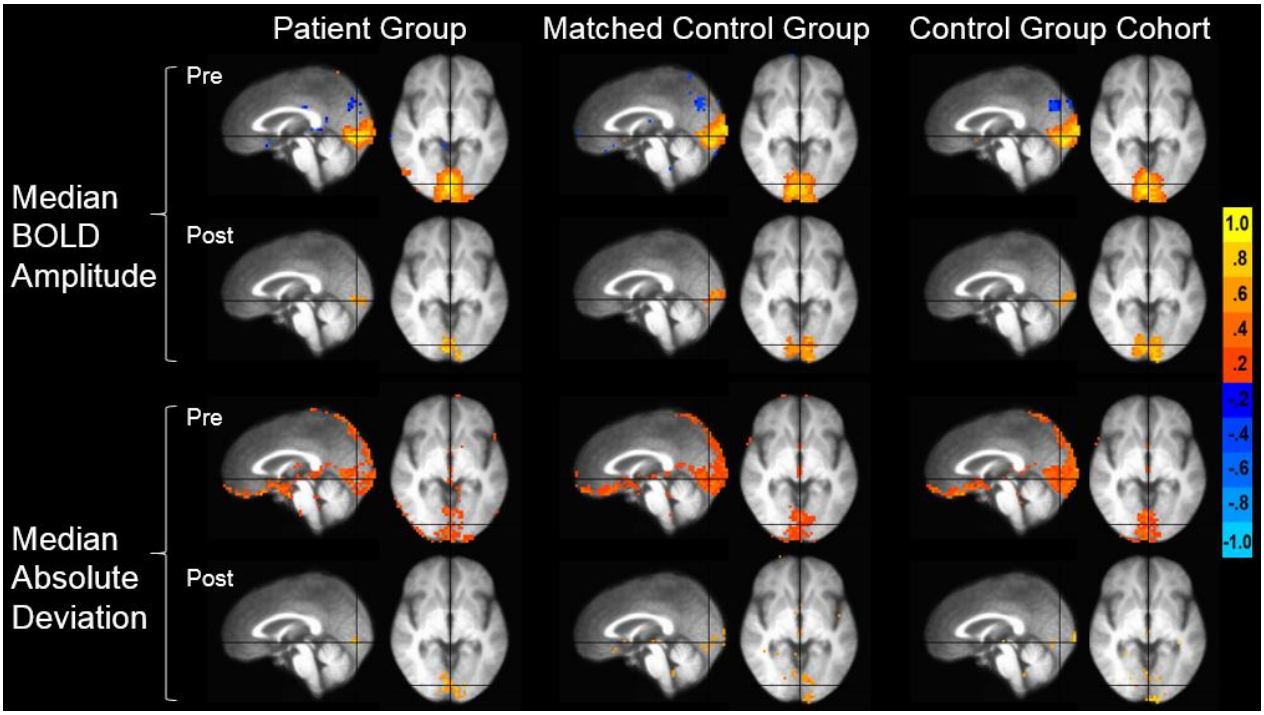

Figure 7
Scaling-induced Changes in Activation Extent and Variability

Median visual stimulation BOLD percent signal change≥0.50 before scaling in the top row and after scaling in the bottom row for all three groups. Median absolute deviation≥0.50 of the unscaled visual stimulation BOLD percent signal change in the top row and after scaling in the bottom row. (This value was chosen as it represents a large enough magnitude to include a sufficient number of voxels for meaningful demonstration of scaling effects (e.g., a threshold of median BOLD changes≥1 would let too few or no voxels pass post-scaling in either parameter), though voxels in regions of deactivation are excluded because their values are too small.) The scale indicates β values. Images are in radiological orientation (left=right) and displayed on the axial z=-2 slice of the group-averaged T1-weighted image in Talairach space. Crosshair is included for comparison with other figures.

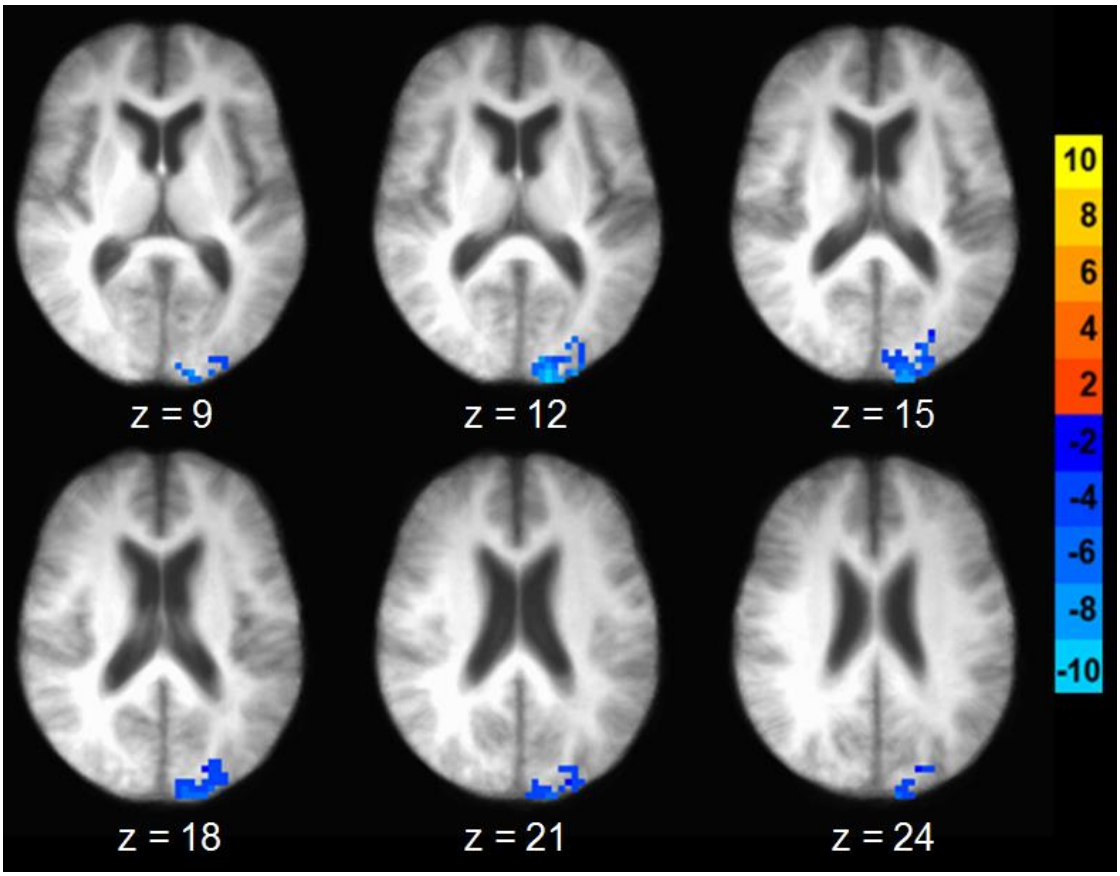

Figure 8
Cluster of Significant Scaling Effects between Groups

A whole-brain Wilcoxon-Mann-Whitney rank sum test examining the scaled visual stimulation BOLD percent signal change of the control vs patient group revealed a cluster in left middle occipital gyrus, extending into cuneus and Brodmann Area 18. Shown are the Wilcoxon rank-sum statistics at a voxel-wise $p<.05$ (two-tailed, cluster family-wise error corrected at $\alpha<.05$, scale indicates the normalized Wilcoxon rank-sum statistics Z). Statistical image is in radiological orientation (left=right) and displayed on axial slices of the group-averaged T1-weighted image in Talairach space. Crosshair is included for comparison with other figures.